surface. Three of the four patients (Patients 1, 3, and 4) had previously undergone allogeneic grafting, which had failed within one year after surgery, despite systemic and local immunosuppression with cyclosporine (trough levels of 50 to 100 ng per milliliter).

Surgical procedures for all cell-sheet autografts were performed by the same surgeon. A complete ophthalmologic examination included measurement of best corrected visual acuity, slit-lamp biomicroscopy, tonometry, and indirect ophthalmoscopy and was performed in all patients every two to four weeks during the follow-up period, starting two weeks after transplantation. The assessments of visual outcomes were carried out by investigators who were not involved in performing the procedures and were not informed about which eye underwent transplantation or whether the assessment was preoperative or postoperative.

CULTURE AND FABRICATION OF AUTOLOGOUS ORAL MUCOSAL EPITHELIAL-CELL SHEETS

After each patient's oral cavity was sterilized with topical povidone-iodine, a 3-by-3-mm specimen of oral mucosal tissue was surgically excised from the interior buccal mucosal epithelium while the patient was under local anesthesia with xylocaine (Fig. 1A). Oral mucosal epithelial cells were collected by removing all epithelial layers after treatment with dispase II (3 mg per milliliter, Roche), at 37°C for one hour. Collected materials were placed in trypsin and EDTA for 15 minutes to form single-cell suspensions. Temperature-responsive cell-culture inserts (CellSeed) were prepared with the use of commercial cell-culture inserts (Falcon, Becton Dickinson) according to specific procedures described previously.[22] The temperature-responsive polymer poly(*N*-isopropylacrylamide), which reversibly alters its hydration properties with temperature, is chemically immobilized in thin films on cell-culture surfaces, facilitating cell adhesion and growth in normal culture conditions at 37°C. Reducing the temperature of the culture below 30°C causes this surface to hydrate and swell rapidly, prompting complete detachment of adherent cells without the use of typical proteolytic enzymes or treatment with EDTA. Confluent cell cultures on these surfaces can be conveniently harvested as a single, unsupported contiguous cell sheet, retaining cell-to-cell junctions as well as deposited extracellular matrix on the basal surface of the sheet.[23] Enzyme-free harvest permits the cell sheets to be readily manipulated, transferred, layered, or fabricated, because they adhere rapidly to other surfaces, such as traditional culture plastics,[22] other cell sheets, and tissues in vivo.[19]

To prepare lethally treated feeder layers, subconfluent NIH 3T3 cells were incubated with 16 μg of mitomycin C per milliliter for two hours at 37°C and then trypsinized and seeded onto tissue-culture wells (35-mm diameter, Becton Dickinson) at a density of 2×10^4 cells per square centimeter. Oral epithelial cells were separated from these feeder-layer cells during culture with temperature-responsive cell-culture inserts. We confirmed that multilayered cell sheets were fabricated only in the presence of 3T3 cells in the culture system. After culture in vitro for 14 days, epithelial-cell sheets (23.4 mm in diameter) were harvested by reducing the temperature to 20°C.

For colony-forming assays, treatment with trypsin and EDTA was used to isolate single cells from oral mucosal epithelium. Cells were counted, seeded onto culture dishes (35-mm diameter, Becton Dickinson), and cultured with feeder layers treated with mitomycin C. After cultivation for 10 to 12 days, dishes were fixed and stained with rhodamine B. Colony formation in the entire dish was screened under a dissecting microscope.

Figure 1 (facing page). Transplantation of Autologous Tissue-Engineered Epithelial-Cell Sheets Fabricated from Oral Mucosal Epithelium.

Panel A shows the removal of oral mucosal tissue (3 by 3 mm) from patient's cheek. Isolated epithelial cells are seeded onto temperature-responsive cell-culture inserts. After two weeks at 37°C, these cells grow to form multilayered sheets of epithelial cells. The viable cell sheet is harvested with intact cell-to-cell junctions and extracellular matrix in a transplantable form simply by reducing the temperature of the culture to 20°C for 30 minutes. The cell sheet is then transplanted directly to the diseased eye without sutures. In Panel B (the scale bar represents 50 μm), harvested cell sheets have three to five cell layers and do not resemble the original oral mucosa as shown in Panel C (the scale bar represents 100 μm) as closely as they resemble normal corneal epithelium as shown in Panel D (the scale bar represents 100 μm). Panel E shows a transmission electron micrograph of developed microvilli on the apical surface of the cell sheet. Specimens of human tissue-engineered epithelial-cell sheets harvested by reducing the temperature of the culture are immunostained green with anti–keratin 3 antibodies (Panel F), anti–β_1 integrin antibodies (Panel G), and anti-p63 antibodies (Panel H). The nuclei in Panels F, G, and H are shown in red. The scale bars represent 50 μm in Panels F, G, and H. The specimens in Panels B, C, and D are stained with hematoxylin and eosin.

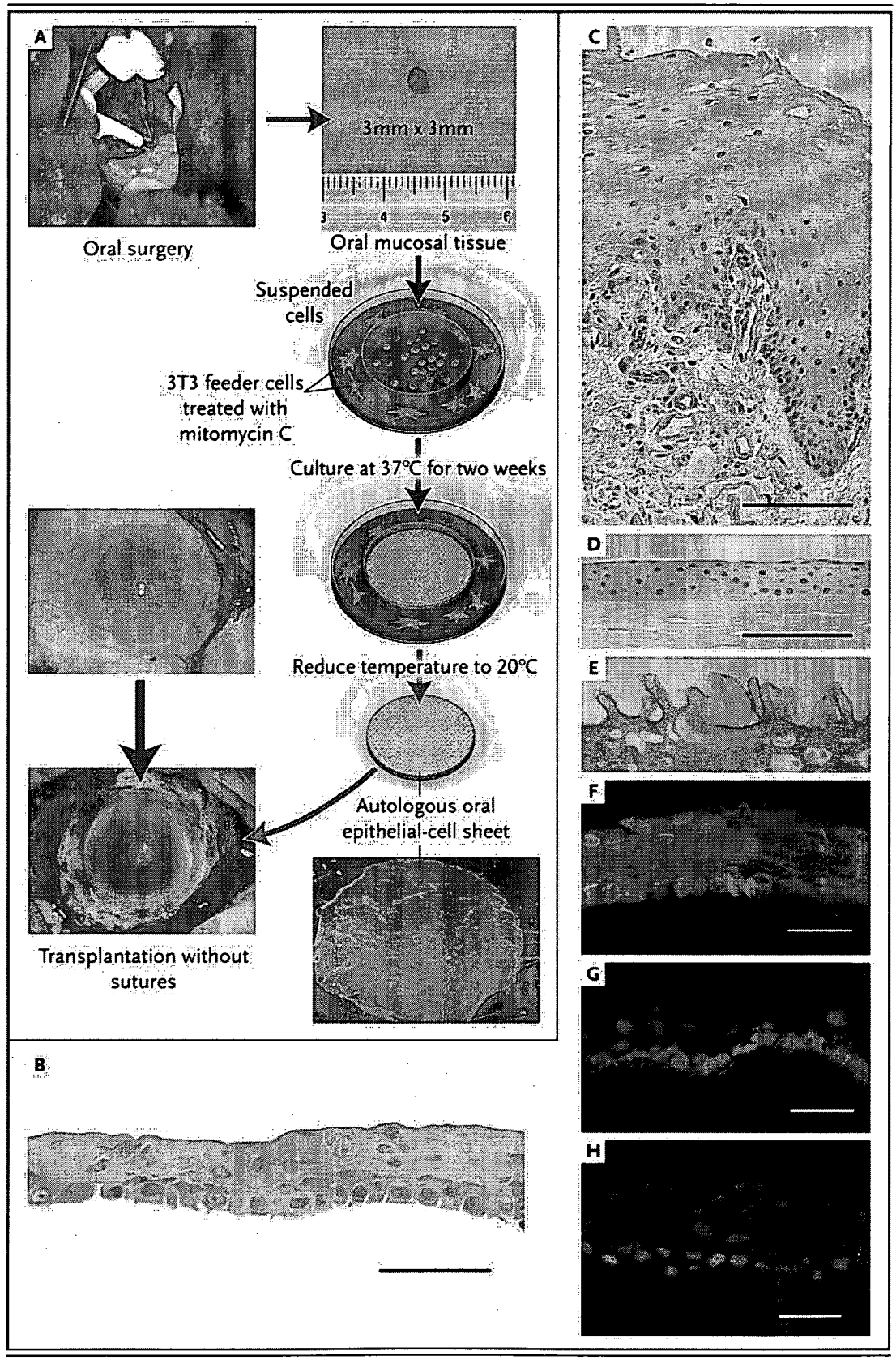
A
Oral surgery
3mm x 3mm
Oral mucosal tissue
Suspended cells
3T3 feeder cells treated with mitomycin C
Culture at 37°C for two weeks
Reduce temperature to 20°C
Autologous oral epithelial-cell sheet
Transplantation without sutures
B
C
D
E
F
G
H

IMMUNOHISTOLOGY

Cryosections from cell sheets were immunostained with monoclonal anti–keratin 3 antibodies (AE5, Progen Biotechnik), anti–β_1 integrin antibodies (P5D2, Santa Cruz Biotechnology), or anti-p63 antibodies (4A4, Santa Cruz Biotechnology) and fluorescein isothiocyanate–labeled or rhodamine-labeled secondary antibodies (Jackson ImmunoResearch Laboratories). Nuclei were costained with Hoechst 33342 (Molecular Probes) or propidium iodide (Sigma). Stained cells were observed using confocal laser scanning microscopy (LSM-510, Zeiss). The same concentration of corresponding normal nonspecific IgG provided negative controls, and native human corneal and limbal tissues were used as positive controls.

TRANSPLANTATION OF CELL SHEETS TO THE EYE

We removed the conjunctival and subconjunctival scar tissue from the cornea up to 3 mm outside the limbus to reexpose corneal stroma (Fig. 2, and a video clip in the Supplementary Appendix, available with the full text of this article at www.nejm.org). Subsequently, the harvested sheet of autologous oral mucosal epithelial cells was placed directly onto the exposed transparent stromal bed as described previously.[6,23] No sutures were required. The grafted corneal surface was then covered with a soft contact lens for protection during healing. After surgery, topical antibiotics (0.3 percent ofloxacin) and steroids (0.1 percent betamethasone) were initially applied four times a day and then tapered to three times a day. During the first week after surgery, betamethasone (1 mg per day) was administered orally to reduce postoperative inflammation. One month after surgery, the administration of topical corticosteroids was changed from 0.1 percent betamethasone to 0.1 percent fluorometholone. Because the patients had severe dry eye, proper wound healing could not be expected without tear supplementation. Preservative-free artificial tears were frequently used, and the puncta lacrimale of all the patients were occluded to increase tear retention.

RESULTS

CHARACTERIZATION OF TISSUE-ENGINEERED EPITHELIAL-CELL SHEETS

We compared cultured autologous oral mucosal-cell sheets with endogenous tissue both functionally and phenotypically. Oral mucosal epithelial cells cultured under these culture conditions resemble corneal epithelium, with three to five cell layers, small basal cells, flattened middle cells, and polygonal and flattened superficial cells (Fig. 1B), more than they resemble native oral mucosal epithelium (Fig. 1C), which is much thicker than corneal epithelium (Fig. 1D). The optical transparency of harvested cell sheets was equal to that of corneal epithelial-cell sheets originating from limbal stem cells (data not shown).[23]

Ultrastructural examination revealed an architecture of well-structured, compact, multilayered cell sheets with the expected microstructures of the native cells, including microvilli (Fig. 1E), tight junctions, desmosomes, and basement membrane. Such morphologic characteristics are similar to those of corneal epithelium in vivo. Native corneal epithelial cells and oral mucosal epithelial cells express keratin 3 as a characteristic phenotypic marker, and harvested epithelial-cell sheets also express keratin 3 (Fig. 1F).

The mean (±SE) colony-forming efficiency, calculated as the ratio of the number of stem or progenitor cells that can produce colonies to the total number of cells in the harvested tissue, was 2.1±0.9 percent for all four patients (with measurements performed in triplicate in each patient), confirming the presence of progenitor cells among the isolated oral mucosal epithelial cells. Correspondingly, β_1 integrin, reported to be an epithelial stem-cell and progenitor-cell marker[24] susceptible to digestion by trypsin, remained intact in the basal cells (Fig. 1G). The basal cells in the multilayered cell sheets also express p63 (Fig. 1H), a putative epithelial stem-cell marker.[25]

CLINICAL RESULTS OF TRANSPLANTATION OF THE CELL SHEET TO THE CORNEAL SURFACE

Attachment of the cell sheet to the stromal bed was spontaneous and uniform (Fig. 2, and video clip in the Supplementary Appendix). Within several minutes after placement without sutures, the grafted cell sheets remained intact and stably bound to the stromal surfaces, even after the extensive application of eyedrops. This observation is consistent with previous experiments with rabbit models, in which transplanted sheets of oral mucosal epithelial cells readily resisted outward displacement when the perimeters were pulled with forceps.

Immediately after surgery, the transplanted corneal surface was clear and smooth, without observable vascularization. Within one week, slit-lamp ex-

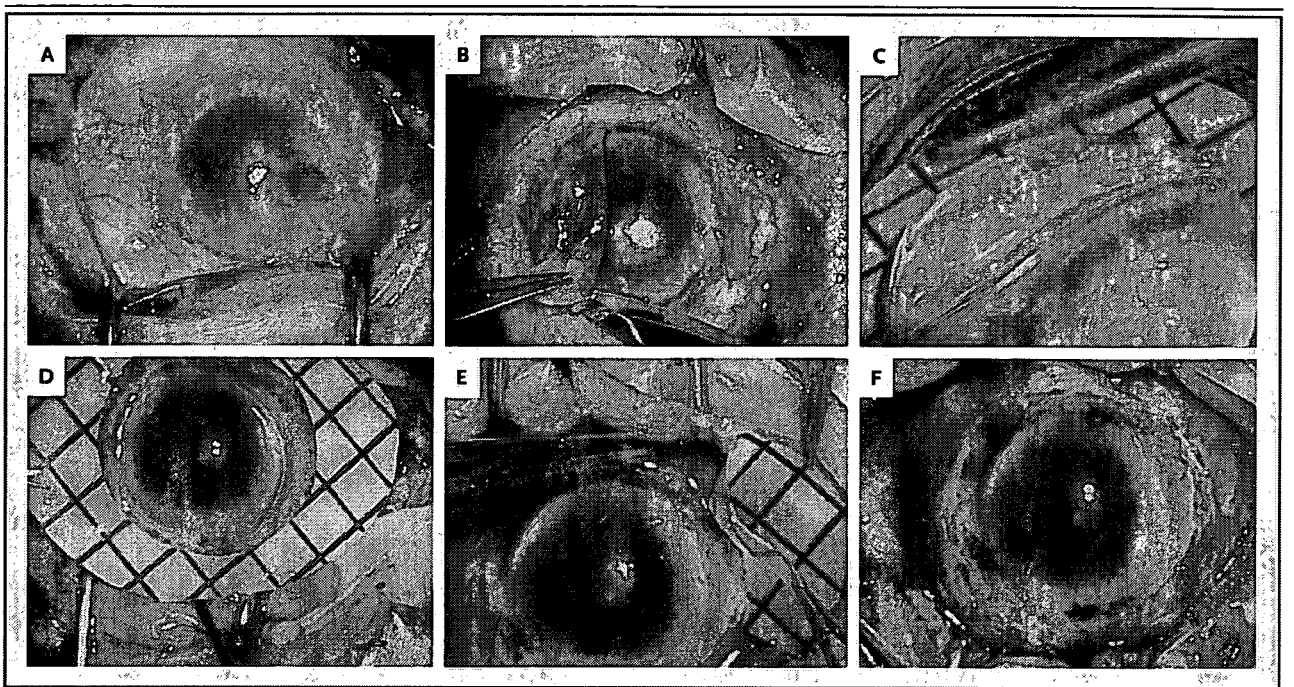

Figure 2. Transplantation Procedures for Tissue-Engineered Autologous Epithelial-Cell Sheets.
Preoperatively, the entire corneal surface was covered by conjunctival tissue with neovascularization (Panel A). In Panel B, conjunctival tissue over the cornea is surgically removed to reexpose transparent corneal stroma. Then, the sheet of tissue-engineered epithelial cells is harvested from a temperature-responsive culture insert with the use of a doughnut-shaped supporter ([black-and-white squares] Panel C) and placed on the stromal bed (Panel D). The sheet adheres to corneal stroma in a few minutes without sutures, and the supporter is removed (Panel E), leaving the cell sheet on the stroma (Panel F). A video clip can be viewed in the Supplementary Appendix, available with the full text of this article at www.nejm.org.

amination with fluorescein sodium staining showed complete reepithelialization of the corneal surface in all four eyes, revealing the tight junction–mediated barrier function. Corneal transparency was restored without any defects of the corneal epithelium. In all eyes, stromal vascularization gradually recurred in the peripheral cornea but not in the central zone. This vascularization was unlike subepithelial vascularization accompanied by conjunctival ingrowth, since it was localized to the deeper stroma and did not show the abnormally high fluorescein permeability characteristic of conjunctival epithelium.

During a mean follow-up period of 14 months, corneal transparency was maintained (Fig. 3 and Table 2). Maximally improved visual acuity was obtained 6, 2, 10, and 8 weeks after transplantation for Patients 1 through 4, respectively, and became stable thereafter. The length of time until visual acuity improved seemed to correspond to the length of time until the corneal stroma became less opaque. No complications were observed.

DISCUSSION

Our study shows that tissue-engineered cell sheets from autologous oral mucosal epithelium may serve as effective substitutes for allografts of limbal tissue in the reconstruction of the corneal and limbal surfaces. Four patients (four eyes) were consecutively treated with this approach, and corneal transparency was restored and postoperative visual acuity improved remarkably (Table 2). During the follow-up period, all corneal surfaces remained transparent, and there were no serious complications.

We developed this strategy on the basis of several observations from cell biology and medicine. First, in vivo oral mucosal epithelium expresses keratin 3, which is also expressed by the corneal epithelium but not by the epidermis.[1,27] Second, the excision of a small piece of oral mucosal tissue from the patient is straightforward, and the resulting wound heals within several days without incident or scarring. Third, transplantation of autologous

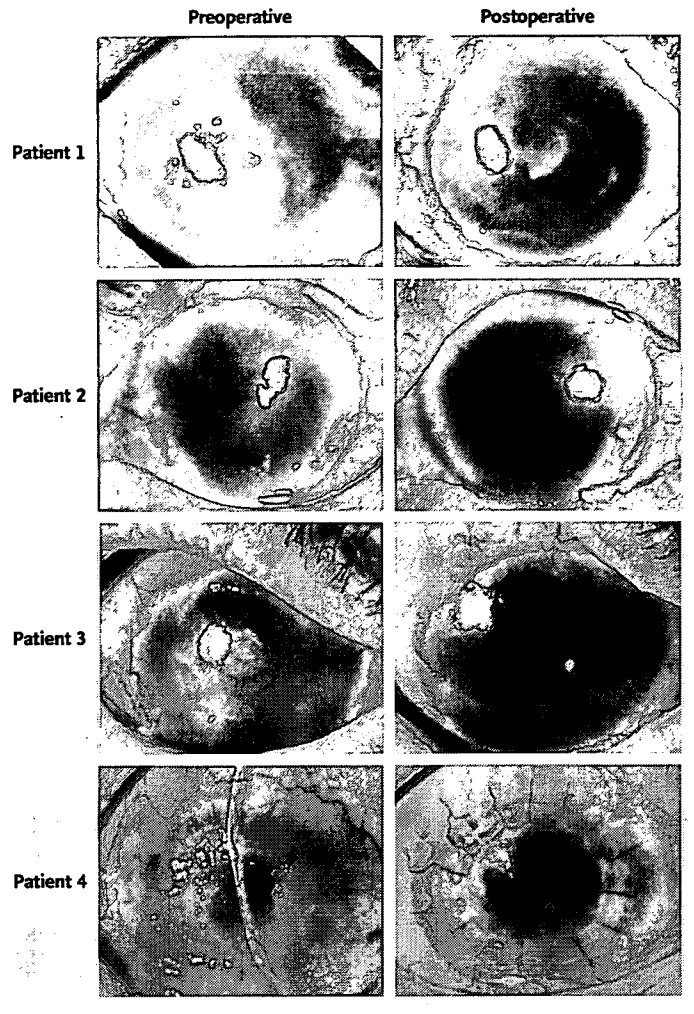

Figure 3. Eyes of Patients before and after Transplantation of Sheets of Tissue-Engineered Autologous Epithelial Cells.

These photographs were taken just before transplantation of the cell sheets and postoperatively at 13, 14, or 15 months.

buccal mucosal grafts directly onto ocular surfaces was previously reported in human patients[28] for the purposes of treating corneal ulcers, corneal perforations, and lid abnormalities (e.g., marginal entropion and trichiasis); these grafts are not useful for improving vision, since they contain opaque subepithelial fibrous tissue. In contrast, the transparency of carrier-free sheets of tissue-engineered epithelial cells fabricated from oral mucosal epithelial cells is similar to the transparency of corneal epithelial-cell sheets originating from limbal stem cells.[23]

Reconstruction with autologous oral mucosal epithelial cells offers substantial clinical advantages over allogeneic transplantation for treating severe diseases such as the Stevens–Johnson syndrome and ocular pemphigoid. It averts the risks of allogeneic immunorejection and immunosuppression. Severe tear-film and lid abnormalities often associated with these diseases continue to be a challenge, since immunologically driven inflammation of the ocular surface persists chronically in these patients.

Although decisive epithelial stem-cell markers that could provide evidence of the presence of these stem cells in grafted cell sheets have not yet been established,[29] results from colony-forming assays for oral mucosal epithelium show that excised oral tissue contains epithelial stem cells or at least progenitor cells. Since ocular surfaces that have been grafted with cell sheets retain their transparency for more than one year, and because the life spans of transient amplifying cells (cells committed to epithelial differentiation) are believed to be less than one year,[30] we conclude that progenitor cells with the potential to differentiate into new corneal epithelial phenotype are present in autografts of cell sheets.

Conjunctival epithelial cells invade the cornea after allogeneic transplantation because of the gradual depletion of allogeneic corneal epithelial cells due to epithelial rejection or stem-cell depletion.[31-33] It is unknown whether this also applies to autologous transplants. In the four eyes we studied, limited stromal vascularization occurred within a few months after transplantation of the cell sheet and reached a stable state within six months, with no appreciable growth thereafter. This stromal vascularization was observed only beneath cell sheets on peripheral corneas and should be distinguished from the subepithelial neovascularization accompanied by conjunctival ingrowth that results from the stem-cell loss associated with allografts, which occurs several months after transplantation. This finding suggests that grafted oral mucosal epithelial cells remained on the ocular surface.

It is possible that the reduction in host immunologic reactions associated with the grafting of autologous cells may minimize epithelial rejection, but further study is needed. The limited stromal neovascularization that we observed is probably caused by angiogenic factors secreted from tissue-engineered epithelial-cell sheets fabricated from oral mucosal epithelial cells originally located in

Table 2. Surgical Outcome in Four Patients Who Received Transplants of Tissue-Engineered Autologous Oral Mucosal-Cell Sheets.

Patient No.	Best Corrected Visual Acuity in Damaged Eye		Corneal Opacity (Grade)*			Complication	Months of Follow-up
	Preoperative†	Postoperative	Preoperative	1 Month after Surgery	At Last Observation		
1	Counting fingers	20/100	3	2	1	None	15
2	20/2000	20/25	3	1	1	None	14
3	Hand motion	20/300	3	1	1	None	14
4	20/2000	20/50	3	1	1	None	13

* The extent of corneal opacity was graded by three masked observers on the basis of the slit-lamp examination with a previously described system[26] and modifications for ocular-surface diseases. Grade 0 indicates clear or trace haze, grade 1 mild opacity, grade 2 moderately dense opacity partially obscuring details of the iris, and grade 3 severely dense opacity obscuring details of the intraocular structure. Grading is based on the opacity observed in all corneal layers, including epithelium, stroma, and endothelium.

† The visual acuity of patients who could not read a visual-acuity chart at a distance of 0.5 m was assessed by asking whether they could see the number of fingers held up by the examiner. If they could not, visual acuity was assessed by the patient's ability to see hand movement by the examiner.

vivo on the substantia propria, which is rich in vessels. However, the production of antiangiogenic factors such as thrombospondin by keratocytes[34] may limit vascularization to peripheral areas.

We observed that the transplanted cell sheets became more transparent and achieved smoother, integrated surfaces on the corneal stroma, further resembling normal corneal epithelium; a plateau was reached one to three months after transplantation. Originally, oral mucosal epithelium, located on substantia propria, is morphologically distinct from corneal epithelium in that it is much thicker and multilayered and has an irregular surface (Fig. 1C). The use of temperature-responsive harvesting allows the grafted carrier-free oral mucosal epithelial cells to interact immediately and directly with patients' corneal stromal keratocytes without interference from cell carriers such as fibrin gel and amniotic membranes.

Our transplantable epithelial-cell sheets used the common 3T3 feeder-layer method originally developed for the production of autologous epidermal-cell grafts[35] and used in the culture of other epithelial cells from various tissue sources, including the limbus.[16] This method has been clinically applied since the 1980s for the treatment of various skin conditions, including burns and giant nevi, although the Food and Drug Administration classifies these grafts as xenografts.

In summary, we have shown that sheets of tissue-engineered epithelial cells fabricated ex vivo from autologous oral mucosal epithelium are effective for reconstructing the ocular surface and restoring vision in patients with bilateral total stem-cell deficiencies. Long-term follow-up and experience with a large series of patients are needed to assess further the benefits and risks of this method, which offers the potential to treat severe ocular diseases that are resistant to standard approaches.

Supported by Grants-in-Aid for Scientific Research (15390530, 16200036, and 16300161), the High-Tech Research Center Program, and the Center of Excellence Program for the 21st Century from the Ministry of Education, Culture, Sports, Science, and Technology in Japan and by the Core Research for Evolution Science and Technology from the Japan Science and Technology Agency.

We are indebted to Professor David Grainger, Colorado State University, and Mr. Joseph Yang, Tokyo Women's Medical University, for their technical review.

REFERENCES

1. Schermer A, Galvin S, Sun TT. Differentiation-related expression of a major 64K corneal keratin in vivo and in culture suggests limbal location of corneal epithelial stem cells. J Cell Biol 1986;103:49-62.
2. Cotsarelis G, Cheng SZ, Dong G, Sun TT, Lavker RM. Existence of slow-cycling limbal epithelial basal cells that can be preferentially stimulated to proliferate: implications on epithelial stem cells. Cell 1989;57:201-9.
3. Thoft RA, Friend J. The X, Y, Z hypothesis of corneal epithelial maintenance. Invest Ophthalmol Vis Sci 1983;24:1442-3.
4. Buck RC. Measurement of centripetal migration of normal corneal epithelial cells in the mouse. Invest Ophthalmol Vis Sci 1985; 26:1296-9.
5. Tseng SC. Concept and application of limbal stem cells. Eye 1989;3:141-57.
6. Nishida K. Tissue engineering of the cornea. Cornea 2003;22:Suppl 7:S28-S34.

7. Kenyon KR, Tseng SC. Limbal autograft transplantation for ocular surface disorders. Ophthalmology 1989;96:709-22.
8. Chen JJ, Tseng SC. Corneal epithelial wound healing in partial limbal deficiency. Invest Ophthalmol Vis Sci 1990;31:1301-14.
9. Dua HS, Azuara-Blanco A. Autologous limbal transplantation in patients with unilateral corneal stem cell deficiency. Br J Ophthalmol 2000;84:273-8.
10. Tsubota K, Satake Y, Kaido M, et al. Treatment of severe ocular-surface disorders with corneal epithelial stem-cell transplantation. N Engl J Med 1999;340:1697-703.
11. Samson CM, Nduaguba C, Baltatzis S, Foster CS. Limbal stem cell transplantation in chronic inflammatory eye disease. Ophthalmology 2002;109:862-8.
12. Ilari L, Daya SM. Long-term outcomes of keratolimbal allograft for the treatment of severe ocular surface disorders. Ophthalmology 2002;109:1278-84.
13. Shimazaki J, Shimmura S, Fujishima H, Tsubota K. Association of preoperative tear function with surgical outcome in severe Stevens-Johnson syndrome. Ophthalmology 2000;107:1518-23.
14. Schwab IR, Reyes M, Isseroff RR. Successful transplantation of bioengineered tissue replacements in patients with ocular surface disease. Cornea 2000;19:421-6.
15. Tsai RJ, Li LM, Chen JK. Reconstruction of damaged corneas by transplantation of autologous limbal epithelial cells. N Engl J Med 2000;343:86-93.
16. Rama P, Bonini S, Lambiase A, et al. Autologous fibrin-cultured limbal stem cells permanently restore the corneal surface of patients with total limbal stem cell deficiency. Transplantation 2001;72:1478-85.
17. Nakamura T, Endo K, Cooper LJ, et al. The successful culture and autologous transplantation of rabbit oral mucosal epithelial cells on amniotic membrane. Invest Ophthalmol Vis Sci 2003;44:106-16.
18. Kinoshita S, Nakamura T. Development of cultivated mucosal epithelial sheet transplantation for ocular surface reconstruction. Artif Organs 2004;28:22-7.
19. Yamato M, Okano T. Cell sheet engineering. Mater Today 2004;May:42-7.
20. Kawasaki S, Nishida K, Sotozono C, Quantock AJ, Kinoshita S. Conjunctival inflammation in the chronic phase of Stevens-Johnson syndrome. Br J Ophthalmol 2000;84:1191-3.
21. Foster CS, Fong LP, Azar D, Kenyon KR. Episodic conjunctival inflammation after Stevens-Johnson syndrome. Ophthalmology 1988;95:453-62.
22. Hirose M, Kwon OH, Yamato M, Kikuchi A, Okano T. Creation of designed shape cell sheets that are noninvasively harvested and moved onto another surface. Biomacromolecules 2000;1:377-81.
23. Nishida K, Yamato M, Hayashida Y, et al. Functional bioengineered corneal epithelial sheet grafts from corneal stem cells expanded ex vivo on a temperature-responsive cell culture surface. Transplantation 2004;77:379-85.
24. Jones PH, Watt FM. Separation of human epidermal stem cells from transit amplifying cells on the basis of differences in integrin function and expression. Cell 1993;73:713-24.
25. Pellegrini G, Dellambra E, Golisano O, et al. p63 Identifies keratinocyte stem cells. Proc Natl Acad Sci U S A 2001;98:3156-61.
26. Fantes FE, Hanna K, Waring GO III, Pouliquen Y, Thompson KP, Salvodelli M. Wound healing after excimer laser keratomileusis (photorefractive keratectomy) in monkeys. Arch Ophthalmol 1990;108:665-75.
27. Moll R, Franke WW, Schiller DL, Geiger B, Krepler R. The catalog of human cytokeratins: patterns of expression in normal epithelia, tumors and cultured cells. Cell 1982;31:11-24.
28. Shore JW, Foster CS, Westfall CT, Rubin PA. Results of buccal mucosal grafting for patients with medically controlled ocular cicatricial pemphigoid. Ophthalmology 1992;99:383-95.
29. Dua HS, Joseph A, Shanmuganathan VA, Jones RE. Stem cell differentiation and the effects of deficiency. Eye 2003;17:877-85.
30. Kinoshita S, Friend J, Thoft RA. Sex chromatin of donor corneal epithelium in rabbits. Invest Ophthalmol Vis Sci 1981;21:434-41.
31. Holland EJ, Schwartz GS. Epithelial stem-cell transplantation for severe ocular-surface disease. N Engl J Med 1999;340:1752-3.
32. Shimazaki J, Kaido M, Shinozaki N, et al. Evidence of long-term survival of donor-derived cells after limbal allograft transplantation. Invest Ophthalmol Vis Sci 1999;40:1664-8.
33. Williams KA, Brereton HM, Aggarwal R, et al. Use of DNA polymorphisms and the polymerase chain reaction to examine the survival of a human limbal stem cell allograft. Am J Ophthalmol 1995;120:342-50.
34. Hiscott P, Sorokin L, Nagy ZZ, Schlotzer-Schrehardt U, Naumann GO. Keratocytes produce thrombospondin 1: evidence for cell phenotype-associated synthesis. Exp Cell Res 1996;226:140-6.
35. Rheinwald JG, Green H. Serial cultivation of strains of human epidermal keratinocytes: the formation of keratinizing colonies from single cells. Cell 1975;6:331-43.

POSTING PRESENTATIONS AT MEDICAL MEETINGS ON THE INTERNET

Posting an audio recording of an oral presentation at a medical meeting on the Internet, with selected slides from the presentation, will not be considered prior publication. This will allow students and physicians who are unable to attend the meeting to hear the presentation and view the slides. If there are any questions about this policy, authors should feel free to call the *Journal*'s Editorial Offices.

Available online at www.sciencedirect.com
SCIENCE DIRECT®
Biochemical and Biophysical Research Communications 337 (2005) 14–21
BBRC
www.elsevier.com/locate/ybbrc

$p57^{Kip2}$ is expressed in quiescent mouse bone marrow side population cells ☆

Terumasa Umemoto [a], Masayuki Yamato [a], Kohji Nishida [b], Joseph Yang [a], Yasuo Tano [b], Teruo Okano [a,*]

[a] *Institute of Advanced Biomedical Engineering and Science, Tokyo Women's Medical University, Tokyo, Japan*
[b] *Department of Ophthalmology, Osaka University Medical School, Osaka, Japan*

Received 31 August 2005
Available online 13 September 2005

Abstract

Hematopoietic stem cells can be accurately identified by the side population (SP) phenotype. It has been previously shown that hematopoietic stem cells are cell cycle arrested, but the mechanisms involved are currently poorly understood. In the present study, results from quantitative real-time RT-PCR show that while SP cells have increased expression of various cyclins and cyclin-dependent kinases, the increased expression of cyclin-dependent kinase inhibitors, in particular $p57^{Kip2}$, is responsible for the observed cell cycle arrest. In addition, gene expression analysis of c-kit^+/Sca-1^+/$Lineage^-$ SP (KSL-SP) cells demonstrates that only $p57^{Kip2}$ shows both higher expression compared to both SP and non-SP cells. Furthermore, immunostaining also demonstrates significantly higher protein expression in KSL-SP cells. These results demonstrate that the maintenance of bone marrow SP cells in G0/G1 may be carefully controlled by $p57^{Kip2}$.

Keywords: Side population; Hematopoietic stem cell; Cell cycle arrest; Cyclin-dependent kinase inhibitor; $p57^{Kip2}$

Hematopoietic stem cells (HSCs) are capable of self-renewal and govern the long-term repopulation of all cell types of the blood forming system [1]. A recently developed technique has employed the differential Hoechst 33342 staining of HSCs to identify a small fraction of bone marrow cells termed "side population" (SP) cells [2]. SP cells have been shown to be highly enriched for HSCs and represent approximately 0.1% of adult nucleated bone marrow cells in mice [3]. This unique ability of SP cells in effluxing Hoechst 33342 is mediated by the ATP-binding cassette transporter G2 (ABCG2), a member of the multiple drug resistance (MDR) family of cell surface transporters [4–6]. SP cells have been found in the hematopoietic compartment of various species [7–10], as well as in other tissues [11–18], demonstrating that the SP phenotype may be a representative characteristic of adult tissue-specific stem cells [19].

A defining feature of adult HSCs is that they are known to reside in the G0/G1 phases of the cell cycle, representing the quiescent state [20], a characteristic which is evidenced by their relatively strong resistance to retroviral infection and cell cycle-specific chemotherapeutic drugs. In somatic cells, the initiation of DNA replication and the associated progression through the cell cycle is known to be controlled by the activity of several classes of cyclin-dependent kinases (Cdks), which are activated by the binding of their respective cyclins. In addition, Cdk activity is carefully regulated by the expression of Cdk inhibitors which can bind to cyclin/Cdk complexes, to prevent cell cycle progression. These Cdk inhibitors are separated into the INK4 family,

☆ *Abbreviations:* HSC, hematopoietic stem cell; SP, side population; ABCG2, ATP binding cassette transporter G2; MDR, multiple drug resistance; Cdk, cyclin-dependent kinase; INK4, inhibitor of cyclin-dependent kinase 4; FACS, fluorescence activated cell sorting; NSP, non-side population; KSL-SP, c-kit^+/Sca-1^+/$Lineage^-$ side population; GAPDH, glyceraldehyde-3-phosphate dehydrogenase.

* Corresponding author. Fax: +81 3 3359 6046.
E-mail address: tokano@abmes.twmu.ac.jp (T. Okano).

0006-291X/$ - see front matter © 2005 Elsevier Inc. All rights reserved.
doi:10.1016/j.bbrc.2005.09.008

which prevents transfer from G1 to S by inhibiting cyclin D/Cdk 4 complex formation; and the Cip/Kip family which inhibits the activities of various cyclin/Cdk complexes.

While the mechanisms governing HSC quiescence are currently not well understood, intuitively it seems that differential expression of proteins involved in mitotic checkpoints may account for the observed cell cycle arrest. It has previously been shown that the induction of the Cdk inhibitors $p15^{INK4b}$ and $p21^{Cip1}$ has an important role in the transforming growth factor (TGF)-β mediated cell cycle arrest in melanoma cells [21]. It was also recently reported that the TGF-β induced cell cycle arrest in hematopoietic progenitor cells was correlated to an increase in $p57^{Kip2}$ expression [22]. $p57^{Kip2}$ has similarly been shown to have an inhibitory effect in the hematopoietic family, by preventing cell cycle progression in human T-lymphocytes [23].

In the present study, we hypothesized that differential expression of various molecules involved in cell cycle checkpoints that regulate progression from G1 to S phase was responsible for the cell cycle arrest observed in bone marrow SP cells. Our findings show that SP cells have increased expression of various cyclins and Cdks, and should therefore have high proliferative potential, but that the increased expression of Cdk inhibitors, in particular $p57^{Kip2}$, blocks the activity of these cyclin/Cdk complexes resulting in the observed quiescent state of HSCs.

Materials and methods

Cell preparation. C57BL/6 mouse (Sankyo Lab Service, Tokyo, Japan) bone marrow cells were obtained by flushing of excised femurs with Hanks' Balanced Salt Solution (Sigma, St. Louis, MO) containing 5% fetal bovine serum (FBS; Moregate Biotech, Queensland, Australia). Cells were collected by centrifugation, followed by disruption of red cells with 0.2% sodium chloride solution. Cells were then washed two times with Dulbecco's phosphate-buffered saline (PBS; Sigma) prior to staining and cell sorting.

Hoechst 33342 exclusion assay using fluorescence activated cell sorting (FACS). Analysis and sorting of SP cells were performed as described previously [17]. Briefly, isolated bone marrow cells were stained with 5 μg/ml Hoechst 33342 (Sigma) at a concentration of 10^6 cells/ml in staining medium (Dulbecco's modified eagle's medium (DMEM) containing 2% FBS and 10 mM Hepes) for 90 min at 37 °C. For inhibition experiments, 50 μM of R (+)-verapamil (Sigma) was added to the staining medium 30 min before the addition of Hoechst 33342. After staining, cells were resuspended in PBS containing 2% FBS and 1 mM Hepes. Prior to analysis and cell sorting, propidium iodide (Sigma) was added at a final concentration of 2 μg/ml, to distinguish between live and non-viable cells. Analysis and cell sorting were then performed using a dual laser fluorescence-activated cell sorter (EPICS ALTRA FACS analysis system, Beckman Coulter, Fullerton, CA).

For the isolation of c-kit$^+$, Sca-1$^+$, Lineage$^-$ SP (KSL-SP) cells, lineage marker-positive cells were first eliminated by magnetic cell sorting (Auto MACS system, Miltenyi Biotec, Bergisch Gladbach, Germany) using the Lineage cell Depletion Kit (Miltenyi Biotec), prior to staining with Hoechst 33342. Lineage$^-$ cells were stained with Hoechst 33342 and then incubated with FITC-conjugated anti-Sca-1 antibody (E13-161.7, BD Biosciences Pharmingen, San Jose, CA) and PE-conjugated anti c-kit antibody (2B8, BD Biosciences Pharmingen) for 30 min on ice. Stained cells were then subjected to sorting by FACS.

Cell cycle analysis. Bone marrow SP cells and total bone marrow cells were pelleted by centrifugation and resuspended in a solution containing 4 mM sodium citrate (pH 7.6), 0.2% Nonidet P-40, and 50 μg/ml propidium iodide. After incubation on ice for 30 min, cell suspensions were treated with 0.25 mg/ml RNase A for 15 min at 37 °C to remove double-stranded RNA. Cells were finally analyzed by flow cytometry at an excitation wavelength of 488 nm.

Gene expression analysis. For gene expression assays, total RNA was obtained from 10,000 SP, non-side population (NSP), or KSL-SP cells using Isogen (Nippongene, Tokyo, Japan) according to the manufacturer's suggested protocol. Single-stranded cDNA was created with the Superscript First-strand System for Reverse Transcriptase-Polymerase Chain Reaction (RT-PCR) (Invitrogen, Carlsbad, CA), and used as PCR templates. Primer pairs and Taqman MGB probes labeled with 6-carboxyfluorescein (FAM) at the 5'-end and non-fluorescent quencher at the 3'-end were designed with the Taqman gene expression assay (Applied Biosystems). Quantitative PCR was performed with 7300 Real-Time PCR System (Applied Biosystems). Thermocycling programs consisted of an initial cycle at 50 °C for 2 min and 95 °C for 10 min, followed by 50 cycles of 95 °C for 15 s and 60 °C for 1 min. All assays were run in duplicate for more than four individual samples. mRNA expression levels were normalized with the expression level of glyceraldehyde-3-phosphate dehydrogenase (GAPDH). To compare mRNA expression between SP, NSP, and KSL-SP cells, the Mann–Whitney rank sum test was applied. Statistics were calculated using SigmaStat 2.0 (SPSS, Chicago, IL).

Immunofluorescence analysis. Cells isolated by FACS were fixed with Methacarn fixation solution, followed by centrifugation onto glass slides. After incubation with 1% bovine serum albumin (Sigma) to block non-specific reactions, cells were incubated with a 1/50 dilution of anti-$p57^{Kip2}$ antibody (E-17, Santa Cruz Biotechnology, Santa Cruz, CA), for 1 h at room temperature, followed by washing three times with PBS. Cells incubated identically with normal goat IgG were used as negative controls. After incubation with a 1/200 dilution of Alexa Fluor 546-conjugated secondary antibodies (Molecular Probes, Eugene, OR) for 1 h at room temperature, cells were again washed three times with PBS. Stained cells were finally counter-stained with 10 μg/ml Hoechst 33342 to visualize cell nuclei, and observed using confocal laser scanning microscopy (TCS-SP, Leica Microsystems AG, Wetzlar, Germany).

Results

The SP phenotype is characterized by low blue and red fluorescence intensity on a density plot due to the efflux of Hoechst 33342 via ABCG2. Mouse bone marrow cells show a typical SP staining pattern, comparable to previously reported results [24,25] (Fig. 1A). Additionally, the SP phenotype could not be detected when bone marrow cells were incubated with verapamil, an MDR inhibitor, prior to staining with Hoechst 33342 (Fig. 1B). Quantitative RT-PCR confirmed that SP cells with low Hoechst-derived fluorescence (Fig. 1A, gated cells) had significantly higher expression of ABCG2, the mediator of the SP phenotype (Fig. 1C), as well as Bmi-1, an important factor in the self-renewal of HSCs [26] (Fig. 1D), compared to NSP cells. These results confirmed that cells with low fluorescence intensity were indeed an SP cell population that is enriched for HSCs. To verify that SP cells represented a quiescent HSC population, cell cycle analysis was performed. Although the cell cycle of total bone marrow cells was promoted with active cell division (Fig. 1E), SP cells were nearly all growth arrested in G0/G1, verifying their quiescent state (Fig. 1F).

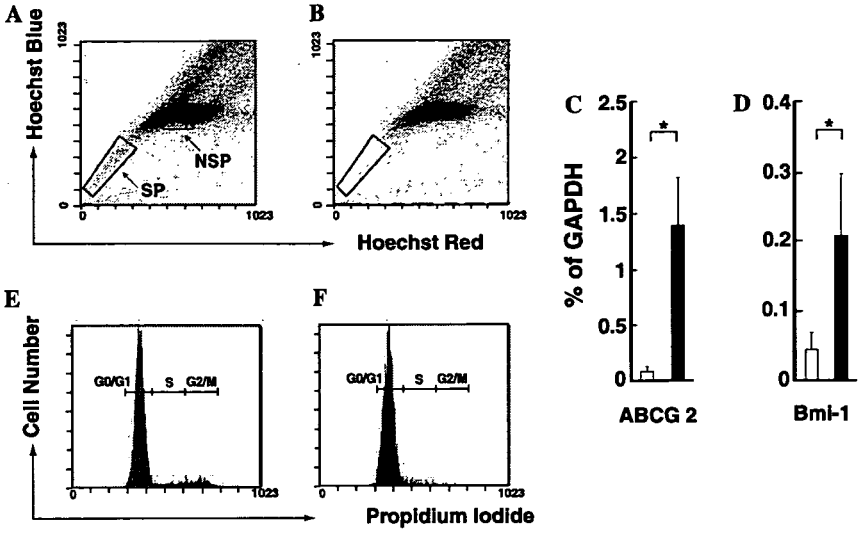

Fig. 1. Mouse bone marrow side population (SP) cells. Bone marrow cells were analyzed for Hoechst 33342 efflux by FACS (A). In the dot plot of (A), cells denoted by each enclosed area were regarded as SP cells or NSP cells for further characterization. When treated with Verapamil, an inhibitor of MDR, Hoechst 33342 efflux was antagonized (B). The expression of the stem cell markers, ABCG2 (C) and Bmi-1 (D), was quantified by real-time RT-PCR. Expression levels were determined from NSP cells: white bar and SP cells: black bar, for each individual mRNA. Data represent mean values from five samples, all performed in duplicate. Error bars indicate the SD (*$p < 0.05$). Additionally, the cell cycle phase in which each individual cell resided from either all viable bone marrow cells (E) or SP cells (F) was detected by flow cytometry.

As SP cells were confirmed to be growth arrested the G1 phase of the cell cycle, we next examined the mRNA expression of cyclin D, cyclin E, Cdk 2, Cdk 4, and Cdk 6, which are required for progression from G1 to S in the cell cycle. Interestingly, all genes examined were more highly expressed in SP cells compared to NSP cells, with significantly greater expression observed for cyclin D1, cyclin D2, and Cdk 4. Therefore, our results indicate that SP cells have high proliferative potential, but that other regulatory mechanisms are likely present to ensure the growth arrest and quiescent state of HSCs (Fig. 2).

As expression of G1- and S-phase Cdk and cyclin mRNAs was higher in SP cells compared to NSP cells, we examined the mRNA expression of the INK4 and Cip/Kip families of Cdk inhibitors. In the INK4 family, both $p15^{INK4b}$ and $p16^{INK4a}$ were barely expressed in either cell fraction (Figs. 3A and B). Additionally, while expression of $p18^{INK4c}$ was higher in SP cells (Fig. 3C), $p19^{INK4d}$ mRNA levels were actually slightly higher in the NSP cell fraction (Fig. 3D). In the Cip/Kip family, both $p21^{Cip1}$ and $p57^{Kip2}$ demonstrated significantly higher expression in SP cells compared to NSP cells, while $p27^{Kip1}$ mRNA expression was higher in NSP cells (Figs. 3E–G).

To investigate the relationship between the observed increase in expression of specific CDK inhibitors and SP cell cycle arrest, bone marrow SP cells were further enriched for

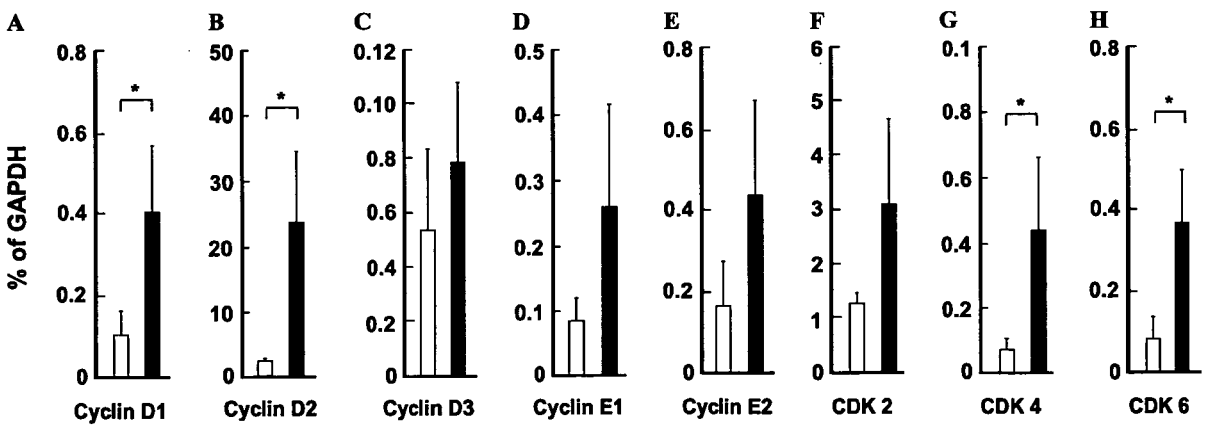

Fig. 2. Expression of cyclin and cyclin-dependent kinase (Cdk) mRNAs in SP and NSP cells. Total RNA was extracted from bone marrow SP cells and NSP cells after FACS, and subjected to real-time quantitative RT-PCR. Relative expression of the selected genes was normalized to that of GAPDH for each sample. mRNA expression of Cyclin D1 (A), Cyclin D2 (B), Cyclin D3 (C), Cyclin E1 (D), Cyclin E2 (E), Cdk 2 (F), Cdk 4 (G), and Cdk 6 (H) is shown. Expression levels were determined from NSP cells: white bar and SP cells: black bar, for each individual mRNA. Data represent mean values from five samples, all performed in duplicate. Error bars indicate the SD (*$p < 0.05$).

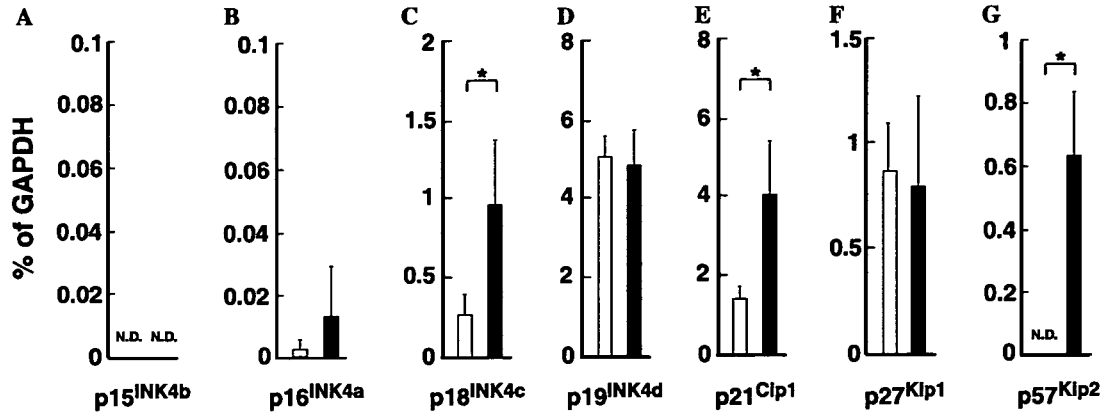

Fig. 3. Expression of cyclin-dependent kinase (Cdk) inhibitor mRNAs in SP and NSP cells. Total RNA was extracted from bone marrow SP cells and NSP cells after FACS, and subjected to real-time quantitative RT-PCR. Relative expression of the selected genes was normalized to that of GAPDH for each sample. mRNA expression of p15 ^{INK4b} (A), p16^{INK4a} (B), p18^{INK4c} (C), p19 ^{INK4d} (D), p21^{Cip1} (E), p27^{Kip1} (F), and p57^{Kip2} (G) is shown. Expression levels were determined from NSP cells: white bar and SP cells: black bar, for each individual mRNA. Data represent the mean value from five samples, all performed in duplicate. Error bars indicate the SD (*$p < 0.05$).

quiescent hematopoietic stem cells by the depletion of lineage-positive cells (Fig. 4A), followed by isolation of c-kit$^+$ and Sca-1$^+$ cells (Figs. 4B and C). mRNA expression of the SP cell marker ABCG2, as well as those CDK inhibitors that showed significantly higher expression in SP cells (p18^{INK4c}, p21^{Cip1}, and p57^{Kip2}), was then examined in the resulting KSL-SP cell population.

Our results demonstrated that KSL-SP cells had much higher expression of ABCG2 and p57^{Kip2} compared to both SP and NSP cells (Figs. 4D and G), but that the expression of both p18^{INK4c} and p21^{Cip1} showed insignificant differences between SP and KSL-SP cells (Figs. 4E and F). To examine p57^{Kip2} protein expression, immunofluorescence was performed with anti-p57^{Kip2} antibodies. Staining visualized with confocal laser scanning microscopy demonstrated that KSL-SP cells had higher expression of p57^{Kip2} protein, compared to NSP cells (Figs. 4H–M). In addition, while KSL-SP cells demonstrated p57^{Kip2} expression that was nearly completely localized to cell nuclei (Figs. 4I, K, and M), the observed low level of p57^{Kip2} in NSP cells showed almost completely cytoplasmic staining (Fig. 4H, J, and L).

These results indicated the possibility that the cell cycle arrest of quiescent bone marrow SP cells was correlated to increased expression of specific Cdk inhibitors, in particular p57^{Kip2}. Therefore, although SP cells may have a strong potential for proliferation due to their increased expression of G1- and S-phase cyclins and Cdks, increased expression of p57^{Kip2} and other Cdk inhibitors was able to induce cell cycle arrest via inhibition of cyclin/Cdk complexes.

Discussion

In the present study, we showed the possibility that the cell cycle arrest observed in bone marrow SP cells, in particular KSL-SP cells, is induced by the Cdk inhibitor p57^{Kip2}. p57^{Kip2} is a well-known member of the Cip/Kip family of Cdk inhibitors that function by binding to cyclin/Cdk complexes to inhibit progression through the cell cycle. Overexpression of p57^{Kip2} has been shown to strongly inhibit somatic cell proliferation [27–29] and p57^{Kip2} has also been shown to be involved in the cell cycle arrest of immature cells in other tissues, such as the retina [30,31] and brain [13]. It was recently reported that TGF-β induced cell cycle arrest of human cord blood derived progenitors required the increased expression of p57^{Kip2} [22]. p57^{Kip2} has also been shown to have genomic imprinting [32,33], which suggests a role in fetal development, as a substantial amount of imprinted genes have critical functions in the control of fetal growth. Therefore, a loss of heterozygosity induces down-regulation and can result in tumor formation [32,34]. It seems likely that p57^{Kip2} is intimately involved in the supervision of cell cycle progression and carefully regulates cell proliferation.

While expression of both p18^{INK4c} and p21^{Cip1} was also significantly higher in SP cells, the difference in the expression of p57^{Kip2} between SP and NSP cells was greatest, with no p57^{Kip2} mRNA detected in NSP cells. Moreover, KSL-SP cells, a cell population more highly enriched for quiescent hematopoietic stem cells, demonstrate a much higher expression of both ABCG2 and p57^{Kip2} than both SP and NSP cells. Hematopoietic stem cells are known to be extremely resistant to various external stresses [35], and the demonstration that the SP cell marker ABCG2 has significantly higher expression in KSL-SP cells compared to both SP and NSP cells further emphasizes that KSL-SP cells are highly enriched for quiescent stem cells.

Previously, Cheng et al. [36] demonstrated that p21^{Cip1} was involved in the maintenance of hematopoietic stem cell quiescence. In the present study, our results also showed that p21^{Cip1} had slightly higher expression in KSL-SP cells. While we cannot exclude the possibility that p21^{Cip1} plays a role in governing the quiescent state of KSL-SP cells, in the previous report by Cheng and colleagues, the authors did

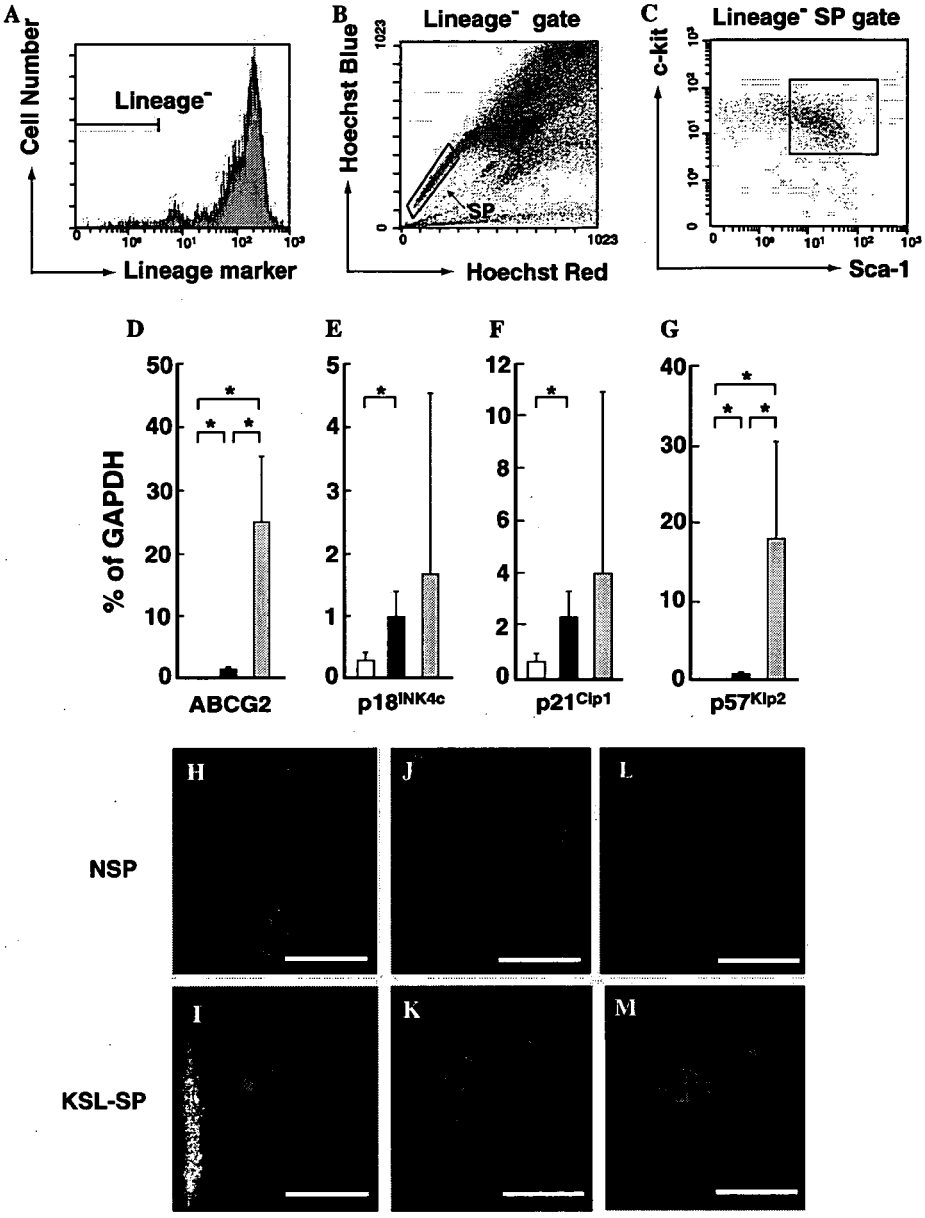

Fig. 4. KSL-SP cells show a high expression of $p57^{Kip2}$. KSL-SP cells were defined by the Lineage$^-$ gate in (A). Lineage$^-$-SP cells (B) were then selected as Sca-1^+ and c-kit^+ (C) for the isolation of KSL-SP cells. mRNA expression of ABCG2 (D), $p18^{INK4c}$ (E), $p21^{Cip1}$ (F), and $p57^{Kip2}$ (G) was then examined using real-time quantitative RT-PCR. Expression levels were determined from NSP cells: white bars, SP cells: black bars, and KSL-SP cells: gray bars, for each individual mRNA. Data represent mean values from four to five samples, all performed in duplicate. Error bars indicate the SD ($*p < 0.05$). Immunofluorescence analysis was performed on NSP cells and KSL-SP cells. Panels represent NSP (H,J,L) and KSL-SP (I,K,M) cells, stained with Hoechst 33342 (H,I), anti-$p57^{Kip2}$ antibody (J,K). (L,M) show merged images. Scale bars represent 20 μm.

not examine the effects of $p57^{Kip2}$. In addition, our findings that $p57^{Kip2}$ expression is specific to SP cells, and in particular KSL-SP cells lead us to believe that $p57^{Kip2}$ is likely the major factor involved in maintaining cell cycle arrest of KSL-SP cells.

Similarly, previous reports have also demonstrated the importance of $p57^{Kip2}$ in the control of the cell cycle. $p57^{Kip2}$ knockout mice often die before birth or else immediately afterwards, due to abnormal apoptosis and morphogenesis [37,38]. In contrast, mice having knockouts for the other Cdk inhibitors examined here, such as $p18^{INK4c}$ [39,40] and $p21^{Cip1}$ [41,42], can survive postnatally. Therefore, $p57^{Kip2}$ seems to be the Cdk inhibitor that is most critically involved in the proper maintenance of cell cycle kinetics.

In many ways, the cancer phenotype resembles a stem cell phenotype, as several cancers are known to express ABCG2, multi-drug resistance protein (MRP), and MDR, and improper regulation of stem cell dynamics is also thought to result in malignant transformation. Loss of function and altered imprinting resulting in altered expression of $p57^{Kip2}$ are known to cause several types of

cancers [43–47] and $p57^{Kip2}$ has been shown to have the strongest tumor suppressor activity in the Cip/Kip family [48]. Therefore, $p57^{Kip2}$ likely has a prominent role in inhibiting cell division.

Interestingly, we also found that SP cells may have a high potential for proliferation due to the increased expression of cyclin D and cyclin E as well as Cdk 2, Cdk 4, and Cdk 6 that are known to promote DNA synthesis and therefore cell cycle progression. Similarly, it has previously been shown that the marker of proliferating cells, Bmi-1, is required for the self-renewal of HSCs, but is also known to decrease the expression of $p16^{INK4a}$ and $p19^{INK4d}$ [26,49,50], and increase telomerase activity [51], which is believed to be indicative of actively proliferating cells. Therefore, it seems that some other regulatory factor, likely $p57^{Kip2}$, is necessary for SP cells to maintain their quiescent state despite their high proliferative potential from increased expression of Bmi-1 as well as, G1- and S-phase cyclins and Cdks.

It has previously been shown that the single characteristic that most accurately identifies a quiescent stem cell population in the bone marrow is the SP phenotype [35]. Bone marrow SP cells have indeed been shown to have the capability for the long-term multi-lineage reconstitution of the hematopoietic system and to reside in a quiescent state in the bone marrow niche [2,35]. It is believed that SP cells from the isolated from the bone marrow by Hoechst 33342 exclusion assays more accurately represent quiescent stem cells than HSCs characterized by other means [35]. Therefore, differences in gene expression between SP and NSP cells isolated from the bone marrow should accurately represent differences between quiescent stem cells and more highly differentiated cells. Because HSCs must govern the long-term maintenance of the entire hematopoietic system, it seems likely that these stem cells require a high proliferative potential to be able to sustain hematopoiesis throughout the host lifetime. However, HSCs must also remain cell cycle arrested in order to carefully regulate this proliferation over time and thus prevent dysfunctions of the hematopoietic system such as various cancers. We therefore hypothesize that the increased expression of the cyclins and Cdks involved in S-phase promotion demonstrates the high proliferative potential of bone marrow SP cells to ensure successful long-term re-population, but that $p57^{Kip2}$ acts to inhibit these cyclin/Cdk complexes and therefore maintain the quiescent state of HSCs and carefully regulate the generation of differentiated progeny.

Previous results have demonstrated that the bone marrow niche in which HSCs reside is critically involved in the maintenance of the quiescent state of the HSCs due to signaling from HSC surface molecules such as Tie-2 [35,52]. It seems likely that the stem cell niche in the bone marrow may be critically involved in inducing $p57^{Kip2}$ expression in order to preserve cell cycle arrest. Further study is needed to identify the system and mechanisms that regulate the expression of $p57^{Kip2}$ such that the proliferation of SP cells, isolated not only from bone marrow, but also other tissues, can be carefully controlled by modifications of gene expression. In the present study, we demonstrate the likely involvement of $p57^{Kip2}$ in inhibiting cell cycle progression of bone marrow SP cells, and thus present a novel mechanism for the maintenance of the quiescent state of HSCs. The careful management of the proliferation of SP cells, which can be found in various tissues, may thus allow for improved applications of cell-based therapies, such as regenerative medicine.

Acknowledgments

This work was supported by Grants-in-Aid for Scientific Research (15390530, 16200036, and 16300161), the High-Tech Research Center Program, the Center of Excellence Program for the 21st Century from the Ministry of Education, Culture, Sports, Science and Technology in Japan, and by the Core Research for Evolution Science and Technology from the Japan Science and Technology Agency.

References

[1] E.A. McCulloch, J.E. Till, The radiation sensitivity of normal mouse bone marrow cells, determined by quantitative marrow transplantation into irradiated mice, Radiat. Res. 13 (1960) 115–125.
[2] M.A. Goodell, K. Brose, G. Paradis, A.S. Conner, R.C. Mulligan, Isolation and functional properties of murine hematopoietic stem cells that are replicating in vivo, J. Exp. Med. 183 (1996) 1797–1806.
[3] M.A. Goodell, M. Rosenzweig, H. Kim, D.F. Marks, M. DeMaria, G. Paradis, S.A. Grupp, C.A. Sieff, R.C. Mulligan, R.P. Johnson, Dye efflux studies suggest that hematopoietic stem cells expressing low or undetectable levels of CD34 antigen exist in multiple species, Nat. Med. 3 (1997) 1337–1345.
[4] S. Zhou, J.D. Schuetz, K.D. Bunting, A.M. Colapietro, J. Sampath, J.J. Morris, I. Lagutina, G.C. Grosveld, M. Osawa, H. Nakauchi, B.P. Sorrentino, The ABC transporter Bcrp1/ABCG2 is expressed in a wide variety of stem cells and is a molecular determinant of the side-population phenotype, Nat. Med. 7 (2001) 1028–1034.
[5] M. Kim, H. Turnquist, J. Jackson, M. Sgagias, Y. Yan, M. Gong, M. Dean, J.G. Sharp, K. Cowan, The multidrug resistance transporter ABCG2 (breast cancer resistance protein 1) effluxes Hoechst 33342 and is overexpressed in hematopoietic stem cells, Clin. Cancer Res. 8 (2002) 22–28.
[6] C.W. Scharenberg, M.A. Harkey, B. Torok-Storb, The ABCG2 transporter is an efficient Hoechst 33342 efflux pump and is preferentially expressed by immature human hematopoietic progenitors, Blood 99 (2002) 507–512.
[7] T. Leemhuis, M.C. Yoder, S. Grigsby, B. Aguero, P. Eder, E.F. Srour, Isolation of primitive human bone marrow hematopoietic progenitor cells using Hoechst 33342 and Rhodamine 123, Exp. Hematol. 24 (1996) 1215–1224.
[8] F.I. Preffer, D. Dombkowski, M. Sykes, D. Scadden, Y.G. Yang, Lineage-negative side-population (SP) cells with restricted hematopoietic capacity circulate in normal human adult blood: immunophenotypic and functional characterization, Stem Cells 20 (2002) 417–427.
[9] M. Feuring-Buske, D.E. Hogge, Hoechst 33342 efflux identifies a subpopulation of cytogenetically normal CD34(+)CD38(−) progenitor cells from patients with acute myeloid leukemia, Blood 97 (2001) 3882–3889.
[10] H. Iwatani, T. Ito, E. Imai, Y. Matsuzaki, A. Suzuki, M. Yamato, M. Okabe, M. Hori, Hematopoietic and nonhematopoietic potentials of Hoechst(low)/side population cells isolated from adult rat kidney, Kidney Int. 65 (2004) 1604–1614.

[11] A. Asakura, Stem cells in adult skeletal muscle, Trends Cardiovasc. Med. 13 (2003) 123–128.
[12] A.J. Alvi, H. Clayton, C. Joshi, T. Enver, A. Ashworth, M.M. Vivanco, T.C. Dale, M.J. Smalley, Functional and molecular characterisation of mammary side population cells, Breast Cancer Res. 5 (2003) R1–R8.
[13] K.A. Jackson, T. Mi, M.A. Goodell, Hematopoietic potential of stem cells isolated from murine skeletal muscle, Proc. Natl. Acad Sci. USA 96 (1999) 14482–14486.
[14] R. Summer, D.N. Kotton, X. Sun, B. Ma, K. Fitzsimmons, A. Fine, Side population cells and Bcrp1 expression in lung, Am. J. Physiol. Lung Cell Mol. Physiol. 285 (2003) L97–L104.
[15] K. Shimano, M. Satake, A. Okaya, J. Kitanaka, N. Kitanaka, M. Takemura, M. Sakagami, N. Terada, T. Tsujimura, Hepatic oval cells have the side population phenotype defined by expression of ATP-binding cassette transporter ABCG2/BCRP1, Am. J. Pathol. 163 (2003) 3–9.
[16] J.X. Zhou, L.W. Jia, Y.J. Yang, S. Peng, Y.J. Cao, E.K. Duan, Enrichment and characterization of mouse putative epidermal stem cells, Cell Biol. Int. 28 (2004) 523–529.
[17] K. Watanabe, K. Nishida, M. Yamato, T. Umemoto, T. Sumide, K. Yamamoto, N. Maeda, H. Watanabe, T. Okano, Y. Tano, Human limbal epithelium contains side population cells expressing the ATP-binding cassette transporter ABCG2, FEBS Lett. 565 (2004) 6–10.
[18] B. Lassalle, H. Bastos, J.P. Louis, L. Riou, J. Testart, B. Dutrillaux, P. Fouchet, I. Allemand, 'Side Population' cells in adult mouse testis express Bcrp1 gene and are enriched in spermatogonia and germinal stem cells, Development 131 (2004) 479–487.
[19] K.D. Bunting, ABC transporters as phenotypic markers and functional regulators of stem cells, Stem Cells 20 (2002) 11–20.
[20] N. Uchida, D. He, A.M. Friera, M. Reitsma, D. Sasaki, B. Chen, A. Tsukamoto, The unexpected G0/G1 cell cycle status of mobilized hematopoietic stem cells from peripheral blood, Blood 89 (1997) 465–472.
[21] V.A. Florenes, N. Bhattacharya, M.R. Bani, Y. Ben-David, R.S. Kerbel, J.M. Slingerland, TGF-beta mediated G1 arrest in a human melanoma cell line lacking p15INK4B: evidence for cooperation between p21Cip1/WAF1 and p27Kip1, Oncogene 13 (1996) 2447–2457.
[22] J.M. Scandura, P. Boccuni, J. Massague, S.D. Nimer, Transforming growth factor beta-induced cell cycle arrest of human hematopoietic cells requires p57KIP2 up-regulation, Proc. Natl. Acad. Sci. USA 101 (2004) 15231–15236.
[23] G. Li, J. Domenico, J.J. Lucas, E.W. Gelfand, Identification of multiple cell cycle regulatory functions of p57Kip2 in human T lymphocytes, J. Immunol. 173 (2004) 2383–2391.
[24] I. Bertoncello, B. Williams, Hematopoietic stem cell characterization by Hoechst 33342 and rhodamine 123 staining, Methods Mol. Biol. 263 (2004) 181–200.
[25] M.A. Goodell, S. McKinney-Freeman, F.D. Camargo, Isolation and characterization of side population cells, Methods Mol. Biol. 290 (2004) 343–352.
[26] I.K. Park, D. Qian, M. Kiel, M.W. Becker, M. Pihalja, I.L. Weissman, S.J. Morrison, M.F. Clarke, Bmi-1 is required for maintenance of adult self-renewing haematopoietic stem cells, Nature 423 (2003) 302–305.
[27] S.A. Kassem, I. Ariel, P.S. Thornton, K. Hussain, V. Smith, K.J. Lindley, A. Aynsley-Green, B. Glaser, p57(KIP2) expression in normal islet cells and in hyperinsulinism of infancy, Diabetes 50 (2001) 2763–2769.
[28] M. Joaquin, R.J. Watson, The cell cycle-regulated B-Myb transcription factor overcomes cyclin-dependent kinase inhibitory activity of p57(KIP2) by interacting with its cyclin-binding domain, J. Biol. Chem. 278 (2003) 44255–44264.
[29] T. Urano, T. Hosoi, M. Shiraki, H. Toyoshima, Y. Ouchi, S. Inoue, Possible involvement of the p57(Kip2) gene in bone metabolism, Biochem. Biophys. Res. Commun. 269 (2000) 422–426.
[30] M.A. Dyer, C.L. Cepko, p57(Kip2) regulates progenitor cell proliferation and amacrine interneuron development in the mouse retina, Development 127 (2000) 3593–3605.
[31] M.A. Dyer, C.L. Cepko, p27Kip1 and p57Kip2 regulate proliferation in distinct retinal progenitor cell populations, J. Neurosci. 21 (2001) 4259–4271.
[32] W.Y. Chung, L. Yuan, L. Feng, T. Hensle, B. Tycko, Chromosome 11p15.5 regional imprinting: comparative analysis of KIP2 and H19 in human tissues and Wilms' tumors, Hum. Mol. Genet. 5 (1996) 1101–1108.
[33] T. Taniguchi, K. Okamoto, A.E. Reeve, Human p57(KIP2) defines a new imprinted domain on chromosome 11p but is not a tumour suppressor gene in Wilms tumour, Oncogene 14 (1997) 1201–1206.
[34] I. Hatada, H. Ohashi, Y. Fukushima, Y. Kaneko, M. Inoue, Y. Komoto, A. Okada, S. Ohishi, A. Nabetani, H. Morisaki, M. Nakayama, N. Niikawa, T. Mukai, An imprinted gene p57KIP2 is mutated in Beckwith–Wiedemann syndrome, Nat. Genet. 14 (1996) 171–173.
[35] F. Arai, A. Hirao, M. Ohmura, H. Sato, S. Matsuoka, K. Takubo, K. Ito, G.Y. Koh, T. Suda, Tie2/angiopoietin-1 signaling regulates hematopoietic stem cell quiescence in the bone marrow niche, Cell 118 (2004) 149–161.
[36] T. Cheng, N. Rodrigues, H. Shen, Y. Yang, D. Dombkowski, M. Sykes, D.T. Scadden, Hematopoietic stem cell quiescence maintained by p21cip1/waf1, Science 287 (2000) 1804–1808.
[37] Y. Yan, J. Frisen, M.H. Lee, J. Massague, M. Barbacid, Ablation of the CDK inhibitor p57Kip2 results in increased apoptosis and delayed differentiation during mouse development, Genes Dev. 11 (1997) 973–983.
[38] P. Zhang, N.J. Liegeois, C. Wong, M. Finegold, H. Hou, J.C. Thompson, A. Silverman, J.W. Harper, R.A. DePinho, S.J. Elledge, Altered cell differentiation and proliferation in mice lacking p57KIP2 indicates a role in Beckwith–Wiedemann syndrome, Nature 387 (1997) 151–158.
[39] E. Latres, M. Malumbres, R. Sotillo, J. Martin, S. Ortega, J. Martin-Caballero, J.M. Flores, C. Cordon-Cardo, M. Barbacid, Limited overlapping roles of P15(INK4b) and P18(INK4c) cell cycle inhibitors in proliferation and tumorigenesis, Embo J. 19 (2000) 3496–3506.
[40] G.I. Kovalev, D.S. Franklin, V.M. Coffield, Y. Xiong, L. Su, An important role of CDK inhibitor p18(INK4c) in modulating antigen receptor-mediated T cell proliferation, J. Immunol. 167 (2001) 3285–3292.
[41] M.L. Santiago-Raber, B.R. Lawson, W. Dummer, M. Barnhouse, S. Koundouris, C.B. Wilson, D.H. Kono, A.N. Theofilopoulos, Role of cyclin kinase inhibitor p21 in systemic autoimmunity, J. Immunol. 167 (2001) 4067–4074.
[42] D.J. Bearss, R.J. Lee, D.A. Troyer, R.G. Pestell, J.J. Windle, Differential effects of p21(WAF1/CIP1) deficiency on MMTV-ras and MMTV-myc mammary tumor properties, Cancer Res. 62 (2002) 2077–2084.
[43] M. Kondo, S. Matsuoka, K. Uchida, H. Osada, M. Nagatake, K. Takagi, J.W. Harper, T. Takahashi, S.J. Elledge, T. Takahashi, Selective maternal-allele loss in human lung cancers of the maternally expressed p57KIP2 gene at 11p15.5, Oncogene 12 (1996) 1365–1368.
[44] J.S. Thompson, K.J. Reese, M.R. DeBaun, E.J. Perlman, A.P. Feinberg, Reduced expression of the cyclin-dependent kinase inhibitor gene p57KIP2 in Wilms' tumor, Cancer Res. 56 (1996) 5723–5727.
[45] J.Y. Shin, H.S. Kim, K.S. Lee, J. Kim, J.B. Park, M.H. Won, S.W. Chae, Y.H. Choi, K.C. Choi, Y.E. Park, J.Y. Lee, Mutation and expression of the p27KIP1 and p57KIP2 genes in human gastric cancer, Exp. Mol. Med. 32 (2000) 79–83.
[46] M. Oya, W.A. Schulz, Decreased expression of p57(KIP2)mRNA in human bladder cancer, Br. J. Cancer 83 (2000) 626–631.
[47] Y. Ito, T. Takeda, M. Sakon, M. Tsujimoto, M. Monden, N. Matsuura, Expression of p57/Kip2 protein in hepatocellular carcinoma, Oncology 61 (2001) 221–225.

[48] M.H. Lee, I. Reynisdottir, J. Massague, Cloning of p57KIP2, a cyclin-dependent kinase inhibitor with unique domain structure and tissue distribution, Genes Dev. 9 (1995) 639–649.
[49] K.S. Smith, S.K. Chanda, M. Lingbeek, D.T. Ross, D. Botstein, M. van Lohuizen, M.L. Cleary, Bmi-1 regulation of INK4A-ARF is a downstream requirement for transformation of hematopoietic progenitors by E2a-Pbx1, Mol. Cell 12 (2003) 393–400.
[50] A.V. Molofsky, R. Pardal, T. Iwashita, I.K. Park, M.F. Clarke, S.J. Morrison, Bmi-1 dependence distinguishes neural stem cell self-renewal from progenitor proliferation, Nature 425 (2003) 962–967.
[51] M. Milyavsky, I. Shats, N. Erez, X. Tang, S. Senderovich, A. Meerson, Y. Tabach, N. Goldfinger, D. Ginsberg, C.C. Harris, V. Rotter, Prolonged culture of telomerase-immortalized human fibroblasts leads to a premalignant phenotype, Cancer Res. 63 (2003) 7147–7157.
[52] K.A. Moore, I.R. Lemischka, "Tie-ing" down the hematopoietic niche, Cell 118 (2004) 139–140.

Rat limbal epithelial side population cells exhibit a distinct expression of stem cell markers that are lacking in side population cells from the central cornea

Terumasa Umemoto[a], Masayuki Yamato[a], Kohji Nishida[b], Chinatsu Kohno[a], Joseph Yang[a], Yasuo Tano[b], Teruo Okano[a,*]

[a] *Institute of Advanced Biomedical Engineering and Science, Tokyo Women's Medical University, 8-1 Kawada-cho, Shinjuku-ku, Tokyo 162-8666, Japan*
[b] *Department of Ophthalmology, Osaka University Medical School, Room E7, Yamadaoka 2-2, Suita, Osaka 565-0871, Japan*

Received 14 October 2005; accepted 18 October 2005

Available online 9 November 2005

Edited by Veli-Pekka Lehto

Abstract The side population (SP) phenotype is shared by stem cells in various tissues and species. Here we demonstrate SP cells with Hoechst dye efflux were surprisingly collected from the epithelia of both the rat limbus and central cornea, unlike in human and rabbit eyes. Our results show that rat limbal SP cells have a significantly higher expression of the stem cell markers ABCG2, nestin, and notch 1, compared to central corneal SP cells. Immunohistochemistry also revealed that ABCG2 and the epithelial stem/progenitor cell marker p63 were expressed only in basal limbal epithelial cells. These results demonstrate that ABCG2 expression is closely linked to the stem cell phenotype of SP cells.

Keywords: Corneal epithelium; Limbal epithelium; Stem cell; Side population; ABCG2

1. Introduction

Previous studies using colony forming studies and label-retaining cell assays have suggested that corneal epithelial stem cells reside in the basal layer of the limbal epithelium [1,2], which is located at the transitional zone between the central cornea and the peripheral bulbar conjunctiva. These stem cells are thought to allow for the proper renewal of the corneal epithelium by generating transient amplifying (TA) cells that migrate, proliferate, and differentiate to replace lost or damaged corneal epithelial cells [3–5]. Recently, several researchers, including our group have succeeded in the clinical transplantation of constructs generated from expanded limbal epithelial cells to treat human patients [6–11]. Additionally, because of the highly limited and well characterized localization of corneal epithelial stem cells to the limbus, the corneal epithelial system has been a model system for epithelial stem cell research [12]. However, due to the absence of definite biological markers, the unequivocal identification and isolation of epithelial stem cells within these populations remain elusive.

*Corresponding author. Fax: +81 3 3359 6046.
E-mail address: tokano@abmes.twmu.ac.jp (T. Okano).

In 1996, Goodell et al. [13] demonstrated that mouse hematopoietic stem cells with long-term multi-lineage reconstitution abilities could be isolated as a side population (SP) based on their unique ability to efflux the DNA-binding dye Hoechst 33342. Recently, SP cells have also been identified in the hematopoietic compartments of different species [14,15], and have been isolated from various other adult tissues including the liver [16], skeletal muscle [17], brain [18], pancreas [19], and lung [20]. These findings suggest that the SP phenotype represents a common feature of adult tissue-specific stem cells. Zhou et al. [21] reported that the ATP-binding cassette transporter, ABCG2 (also known as BCRP-1 or MXR), is a molecular determinant of this SP phenotype in hematopoietic stem cells. Other studies in a wide range of organs have also indicated that the SP phenotype is largely determined by the expression of ABCG2 [16,19,20,22], a member of the multiple drug resistance (MDR) family of membrane transporters. Taken together, these previous results suggest that the SP phenotype may be an extremely useful tool for the identification of stem cells from various tissues.

Recently, we reported that both the human and rabbit limbal epithelium contains SP cells expressing ABCG2, while SP cells could not be detected in the epithelium of the central cornea [23,24]. In the present study, we investigated the presence of SP cells in both the limbal and corneal epithelium of the rat by fluorescence-activated cell sorting (FACS) and discovered that while cells with the SP phenotype could also be detected in the rat central cornea, only SP cells isolated from the limbal epithelium demonstrated a distinct expression of stem cell markers.

2. Materials and methods

2.1. Cell preparation

Corneoscleral rims were obtained from Wistar rats (8 weeks old, male) and New Zealand white rabbits (2.0 kg, male). Limbal tissues were obtained with scissors, and 2.0 mm-diameter portions of rat corneas and 8.0 mm-diameter portions of rabbit central corneas were obtained by trephination (Fig. 1). Excised tissues from the limbus and central corneas were treated with Dulbecco's modified Eagle's medium (DMEM) containing 120 U/ml dispase II (Godo Shusei, Tokyo, Japan) at 37 °C for 1 h. Epithelial cells were then separated under a dissecting microscope and treated with 0.25% trypsin/1 mM EDTA solution (Invitrogen, Carlsbad, CA) for 20 min at 37 °C, to create single cell suspensions and enzymatic activity was stopped by adding an equal volume of DMEM containing 10% fetal bovine serum (FBS; Moregate BioTech, Queensland, Australia).

0014-5793/$30.00
doi:10.1016/j.febslet.2005.10.047

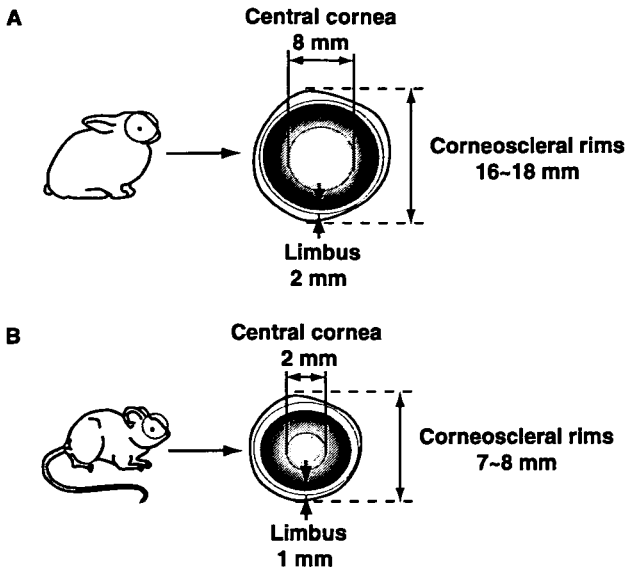

Fig. 1. Isolation of limbal and corneal tissues. (A) Approximately 16–18 mm diameter tissues including cornea, limbus and conjunctiva were isolated from New Zealand white rabbits. From these tissues, 2 mm regions of the limbus were harvested with scissors and 8 mm diameter portions of central corneas were obtained by trephination. (B) In rat tissues, 7–8 mm diameter tissues were isolated and 1 mm limbal tissues and 2 mm diameter portions of central corneas were obtained.

2.2. Hoechst 33342 exclusion assay using fluorescence-activated cell sorting

Single cells isolated from both the limbal epithelium and the corneal epithelium were subjected to FACS using previously described procedures [24].

2.3. Gene expression analysis

Gene expression analyses were conducted using real-time quantitative RT-PCR, as previously described [24].

2.4. Immunohistochemistry

Limbal and corneal tissues were fixed in 10% neutral buffered formalin (Wako Pure Chemicals, Tokyo, Japan) and routinely processed into paraffin-embedded sections. Immunostaining was then performed using the DAKO LSAB kit/HRP (DAB) (Dako Cytomation, Glostrup, Denmark). Briefly, endogenous peroxidase activity was blocked with Peroxidase Blocking Reagent, DAKO S 2001 (Dako). After incubation with 1% bovine serum albumin to block non-specific reactions, sections were incubated with either a 1/200 dilution of anti-ABCG2 antibody (5D3, MBL, Aichi, Japan) or a 1/200 dilution of anti-p63 antibody (4A4, Santa Cruz Biotechnology Inc., Santa Cruz, CA) for 1 h at room temperature, followed by three washes with Dulbecco's phosphate buffered saline (PBS). Sections incubated identically with normal mouse IgG were used as negative controls. After incubation with horseradish peroxidase-conjugated secondary antibodies (Dako) for 30 min at room temperature, the sections were again washed 3 times with PBS. Finally, color development was performed using DAKO ENVISION kit/HRP (DAB) (Dako) and stained sections were visualized using light microscopy.

3. Results

Using FACS, a distinct population of cells with a low Hoechst 33342 blue/red fluorescence was isolated from both rabbit and rat limbal epithelial cells (Fig. 2A and E) analogously to previously reported results for both human and rabbit eyes [23–26], with dye efflux inhibited by treatment with verapamil,

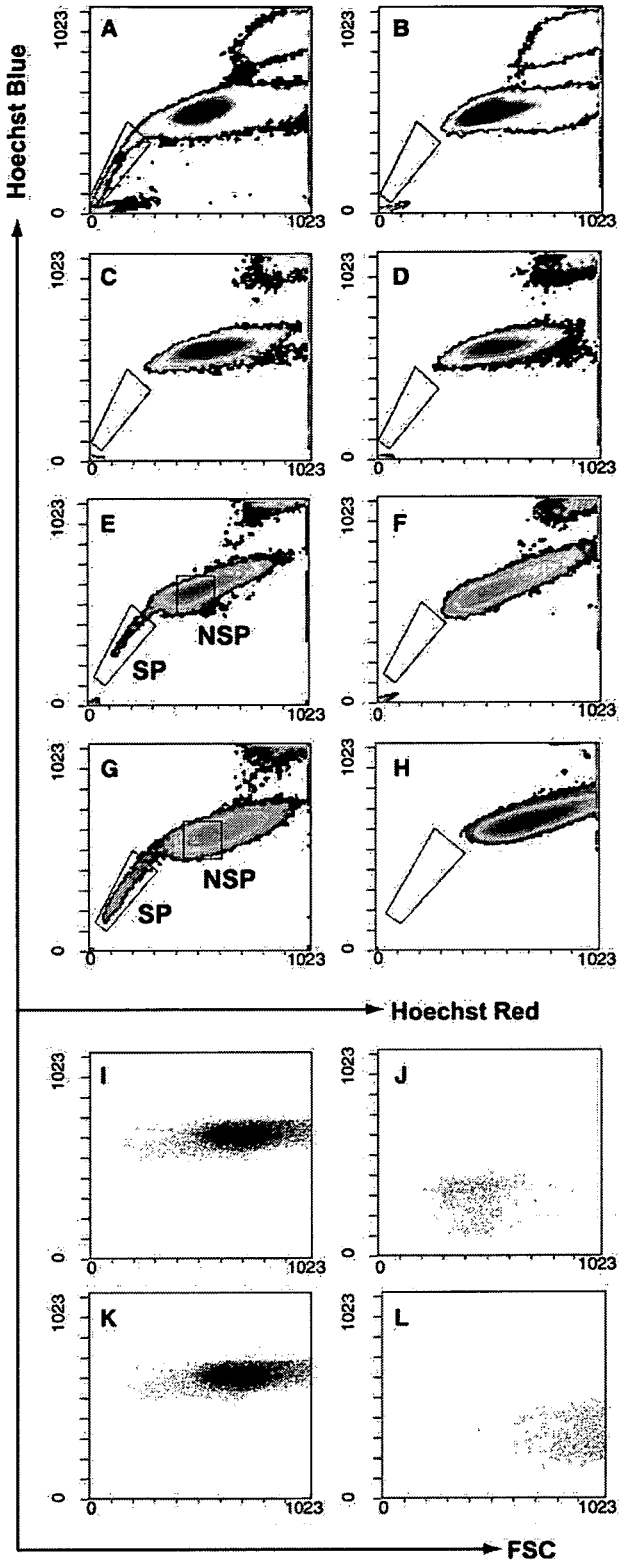

Fig. 2. Hoechst 33342 staining in rabbit and rat limbal and corneal epithelial cells. Epithelial cells were isolated for the cornea and limbus and subjected to Hoechst 33342 exclusion assay. Cells were sorted using FACS and SP cells were detected in the epithelial cells of rabbit limbus (A, B), rabbit cornea (C, D), rat limbus (E, F), and rat cornea (G, H). Dye efflux from SP cells was antagonized by verapamil (B, D, F, H). Forward scattering shows the relative cell size of limbal NSP (I), limbal SP (J), corneal NSP (K) and corneal SP cells (L) in rat. In the density plots of E and G, cells denoted by each enclosed area were regarded as SP and NSP cells for further characterization.

a known inhibitor of Hoechst 33342 dye transport (Fig. 2B and F). The frequency of 0.56% and 0.40% of gated cells for rabbit and rat, respectively, as well as elimination of the SP phenotype by verapamil, was similar to our previously reported results with human eyes [23]. In contrast, cells within the SP gate were barely detected in the corneal epithelium of rabbits (Fig. 2C). However, when epithelial cells from the rat central cornea were subjected to Hoechst 33342 exclusion assays, surprisingly, a significant cell population (4.6% of gated cells) showing the SP phenotype was detected (Fig. 2C). This frequency of rat corneal epithelial SP cells was ten times higher than from the limbal epithelium, but cells showing the SP phenotype were also blocked by treatment with verapamil (Fig. 2H). Forward scatter analyses using FACS also revealed that rat limbal SP cells (Fig. 2J) were smaller in size than both rat limbal NSP cells (Fig. 2I) and rat corneal epithelial NSP cells (Fig. 2K), but that rat corneal epithelial SP cells (Fig. 2L) were much larger than these other cell types.

SP and NSP cells isolated from both the rat limbal epithelium and corneal epithelium were then subjected to real-time quantitative RT-PCR (Fig. 3). Consistent with experimental design, significantly higher expression of ABCG2 mRNA was observed in limbal epithelial SP cells over all other cell fractions (Fig. 3A). In contrast, the expression of ABCG2 could barely be detected in rat corneal epithelial SP cells. These cell fractions were also subjected to gene expression analyses for four common stem cell markers: nestin (Fig. 3B), notch 1 (Fig. 3C), TERT and musashi 1 (data not shown). Significantly higher expression of nestin and notch 1 mRNAs were found in limbal epithelial SP cells compared to limbal epithelial NSP cells as well as both cell fractions isolated from the central corneas. However, gene expression levels of both TERT and musashi 1 were undetectable in all cell fractions (data not shown).

Finally, immunohistochemistry revealed a similar localization of the SP cell marker, ABCG2 with p63, in the rat ocular surface (Fig. 4). p63 is well-known as a marker of epithelial stem and progenitor cells, and p63 positive cells have been previously reported to be localized in the basal layer of the limbal

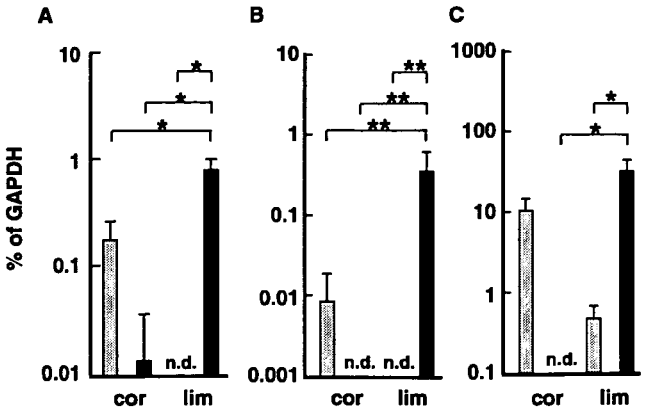

Fig. 3. mRNA analysis of stem cell marker gene expression. Total RNA was extracted from cells isolated by FACS and subjected to real-time quantitative RT-PCR. The relative gene expression of ABCG2 (A), nestin (B), and notch 1 (C) were plotted as a ratio of GAPDH gene expression. Expression levels were detected from NSP cells: gray bars, and SP cells: black bars. Data represent the mean value from three to four independent samples. Error bars indicate the SD ($^{*}P = 0.01$ and $^{**}P < 0.05$, respectively).

epithelium, but not in the central cornea [27]. Our present results demonstrated that the localization of both ABCG2 and p63 were restricted to the basal layer of the limbal epithelium (Fig. 4C and E), and could not be found in any regions of the central corneas (Fig. 4D and F).

4. Discussion

In the present study, we report the isolation of a cell population showing the SP phenotype from rat corneal epithelium and their comparison to SP cells isolated from the limbal epithelium. The SP phenotype is now consistently attributed to various adult tissue-specific stem cells and commonly associated with the functional presence of the ATP-binding cassette transporter, ABCG2 [21,22]. The

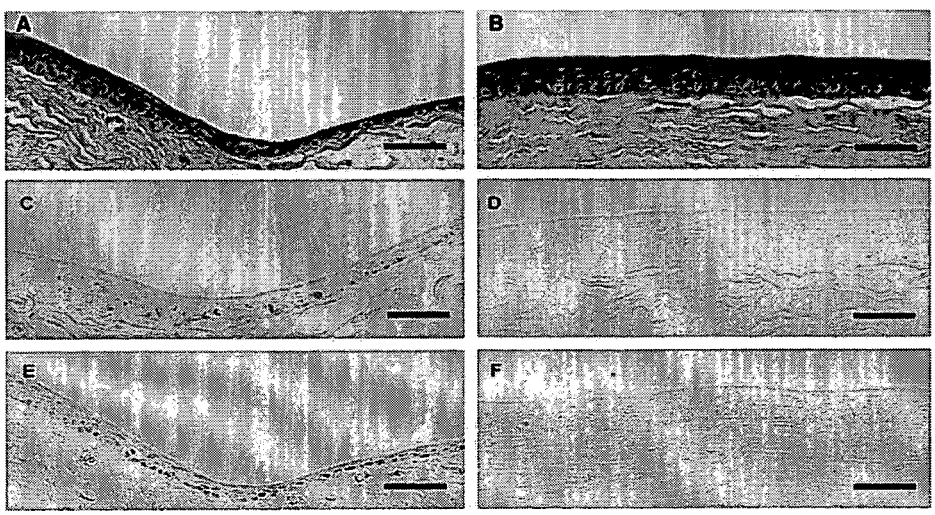

Fig. 4. Immunohistochemistry for ABCG2 and p63 in rat cornea and limbus. The distribution of cells expressing ABCG2 and p63 were examined using immunohistochemistry. Hematoxylin and eosin staining (A, B), and immunostaining with anti-ABCG2 (C, D) and anti-p63 (E, F) antibodies. Left (A, C, E) and right (B, D, F) panels represent rat limbus and cornea, respectively. Scale bars indicate 50 μm.

expression of ABCG2, which is considered a putative marker of the SP phenotype has been reported for cells isolated from numerous tissues, with these cells also exhibiting stem cell-like phenotypes [19,20,22,24]. While our results from FACS have shown that only approximately 0.5% of limbal epithelial cells exhibited the SP cell phenotype regardless of species (Fig. 2A and E) [23,24], immunohistochemistry revealed that a large portion of limbal basal epithelial cells (approximately 10% of total limbal epithelial cells) expressed ABCG2 (Fig. 4C). This apparent discrepancy may be attributed to the transport activity of ABCG2. Limbal basal epithelial cells have relatively little cytoplasmic area, and it is therefore difficult to determine whether ABCG2 molecules were localized to the plasma membranes or in the cytoplasm (Fig. 4C). Since only active ABCG2 transporter present on the cell surface can efflux Hoechst 33342 [20,28], cytoplasmic ABCG2 would be unable to contribute to the observed low Hoechst-derived fluorescence. Additionally, Mogi et al. [28] recently showed that a serine/threonine kinase, Akt, can modulate the SP phenotype by controlling the expression ABCG2, which suggests that ABCG2 function is under strict regulation.

In the present study, while limbal SP cells show higher expression of tissue-specific stem cell markers, in particular ABCG2, compared to the other cell populations examined, these differences in gene expression levels are not as great as observed for both human [23] and rabbit limbal epithelial SP cells [24]. The disparity in the present case is linked to the purity of limbal epithelial SP cells used in the present rat experiments. In the cases of human and rabbit, the central cornea does not contain SP cells that can possibly contaminate the limbal SP population. Additionally, with rat eyes, the significantly smaller size, as well as a lack of the Palisades of Vogt, means that the border between the limbus and central cornea is undefined and difficult to interpret. Therefore, the presence of SP cells in the epithelium of the central cornea inevitably leads to contamination by cells that do not show expression of stem cell markers, causing the relative expression of ABCG2, nestin, and notch 1 to be decreased in the limbal epithelial SP cell fraction that has stem cell-like properties. In contrast to rabbit and human cases, where these factors do not influence the limbal epithelial SP population, differences of approximately 100× in the expression of ABCG2, are considerably greater than the approximately 10× difference observed in the present study, which is a result of this unavoidable contamination. Regarding the relationship between ABCG2 expression and stem cell phenotypes, we have previously shown that SP cells from the mouse bone marrow have approximately 15× higher ABCG2 expression than NSP cells. However, when bone marrow SP cells were further purified for hematopoeitic stem cells by sorting of c-kit$^+$/Sca-1$^+$/Lineage cell marker$^-$ SP cells, this fraction showed 250× greater ABCG2 expression compared with NSP cells [29]. These data suggest the importance of ABCG2 expression for the identification of tissue-specific stem cells using Hoechst 33342 efflux assays.

From the rat limbal epithelium, SP cells also showed an increased expression of the stem cell markers nestin and notch 1, compared to NSP cells from both the limbal epithelium and corneal epithelium, as well as SP cells from the corneal epithelium (Fig. 3). However, even though SP cells were detected in the central cornea, this cell fraction showed significantly lower expression of these stem cell markers compared to limbal epithelial SP cells (Fig. 3).

Nestin is known as a neural stem cell marker [30], but its expression is not limited to neural tissues, and has been recently reported in pancreatic islets [19] and even in the cornea [31]. Specifically in the eyes, retinal SP cells have been reported to exhibit a high expression of nestin mRNA [32]. Notch 1 has also been frequently correlated to a stem cell-like phenotype, by delaying stem cell differentiation via the enhancement of self-renewal in both hematopoietic [33,34] and neural stem cells [35]. The higher expression of notch 1 observed in limbal epithelial SP cells suggests that these cells may indeed resemble other adult stem cells and may indicate a key role of notch 1 signaling in regulating ocular surface homeostasis through well-controlled corneal epithelial turnover. Musashi 1 is another well-recognized neural stem cell marker [36], but its mRNA expression was undetectable in all cell fractions studied, including limbal epithelial SP cells (data not shown), which may imply its specificity to neural tissues. The physiological expression of TERT is highly limited to a very specific number of cell types including proliferating stem cells, reproductive cells, and cancer cells [37,38]. In our experiments, TERT mRNA was not detected in limbal SP cells isolated from normal healthy tissues. Since adult stem cells are considered to be slow-cycling or arrested in the G0/G1 phases of the cell cycle [2,39,40], constitutive expression of TERT is unlikely to be observed in quiescent stem cells. Recent reports have shown that skin epidermal SP cells expressing ABCG2 and putative skin epidermal stem cells exhibiting slow cell cycling are two distinct cell populations [41] and we have also shown that limbal epithelial SP cells with significantly higher expression of ABCG2 represented a quiescent population with stem cell-like properties, without TERT activity [24].

While our results indicate that SP cells isolated from the rat limbal epithelium may constitute a population enriched for stem cells, when SP cells were isolated from rat central corneas, these cells had expression levels of ABCG2 that could be barely detected (Fig. 3A). Immunohistochemistry with anti-ABCG2 antibody also demonstrated that ABCG2 could not be observed in corneal epithelial cells (Fig. 4D). It was recently reported that the human epidermis contains SP cells that do not express ABCG2 [42]. These results imply that a transporter other than ABCG2 may be responsible for the observed Hoechst 33342 efflux in rat corneal epithelial cells. Furthermore, consistent with the absence of ABCG2, rat corneal epithelial SP cells also exhibited similar cell sizes to corneal epithelial NSP cells, and were larger than limbal epithelial SP cells (Fig. 2I–L). It has been noted that stem cells isolated from other tissues such as the skin and hair follicle [43–45] have smaller cell sizes than their more differentiated progeny. The SP cell frequency in rat corneal epithelium (4.6%) was also much higher than in the limbus, as well as results reported for several tissues and organs [13,16,20,23], and the presence of corneal epithelial SP cells in rat eyes were contrary to our previous results for both human [23] and rabbit [24]. Similarly, immunostaining for p63, a known epithelial stem and progenitor cell marker [27], also showed positive staining only in the limbal epithelium and not in the central cornea (Fig. 4E and F). These findings support the theory that even though SP cells were detected in the central corneas of rats, this cell population is distinct from limbal epithelial SP cells and other typical SP cells that show high expression of ABCG2 and are enriched

for tissue-specific stem cells. It is possible that other members of the ABC transporter family may be expressed in corneal epithelial SP cells allowing for the efflux of Hoechst 33342 and therefore the observed SP phenotype, but that these cells lack ABCG2 that is expressed in many tissue-specific stem cells. However, even though it seems likely that corneal epithelial SP cells lack stem cell-like properties, further analysis of the stem cell properties including studies on the capabilities for self-renewal and differentiation are required for a decisive conclusion.

In summary, we have shown that similarly to other species, rat limbal epithelial SP cells show a significantly higher expression of ABCG2 and that these cells also show increased mRNA expression of the stem cell markers nestin and notch 1. However, even with the interesting finding that SP cells may comprise a population enriched for stem cells, the presence of SP cells in the central cornea without ABCG2 expression and seemingly without stem cell-like properties, demonstrates the presence of two distinct SP cell populations in the rat ocular surface. It therefore seems increasingly necessary to confirm the expression of ABCG2 when using SP cells for stem cell research.

Acknowledgments: We appreciate the useful comments and technical criticism of Professor D.W. Grainger (Colorado State University, USA). This work is supported in part by Grants-in-Aid for Scientific Research (16200036 and 16300161), the High-Tech Research Center Program, and the Center of Excellence Program for the 21st Century from the Ministry of Education, Culture, Sports, Science, and Technology in Japan and by the Core Research for Evolution Science and Technology from the Japan Science and Technology Agency.

References

[1] Schermer, A., Galvin, S. and Sun, T.T. (1986) Differentiation-related expression of a major 64K corneal keratin in vivo and in culture suggests limbal location of corneal epithelial stem cells. J. Cell. Biol. 103, 49–62.
[2] Cotsarelis, G., Cheng, S.Z., Dong, G., Sun, T.T. and Lavker, R.M. (1989) Existence of slow-cycling limbal epithelial basal cells that can be preferentially stimulated to proliferate: implications on epithelial stem cells. Cell 57, 201–209.
[3] Kinoshita, S., Friend, J. and Thoft, R.A. (1981) Sex chromatin of donor corneal epithelium in rabbits. Invest. Ophthalmol. Vis. Sci. 21, 434–441.
[4] Thoft, R.A. and Friend, J. (1983) The X, Y, Z hypothesis of corneal epithelial maintenance. Invest. Ophthalmol. Vis. Sci. 24, 1442–1443.
[5] Buck, R.C. (1985) Measurement of centripetal migration of normal corneal epithelial cells in the mouse. Invest. Ophthalmol. Vis. Sci. 26, 1296–1299.
[6] Pellegrini, G., Traverso, C.E., Franzi, A.T., Zingirian, M., Cancedda, R. and De Luca, M. (1997) Long-term restoration of damaged corneal surfaces with autologous cultivated corneal epithelium. Lancet 349, 990–993.
[7] Nishida, K. et al. (2004) Functional bioengineered corneal epithelial sheet grafts from corneal stem cells expanded ex vivo on a temperature-responsive cell culture surface. Transplantation 77, 379–385.
[8] Rama, P., Bonini, S., Lambiase, A., Golisano, O., Paterna, P., De Luca, M. and Pellegrini, G. (2001) Autologous fibrin-cultured limbal stem cells permanently restore the corneal surface of patients with total limbal stem cell deficiency. Transplantation 72, 1478–1485.
[9] Koizumi, N., Inatomi, T., Suzuki, T., Sotozono, C. and Kinoshita, S. (2001) Cultivated corneal epithelial stem cell transplantation in ocular surface disorders. Ophthalmology 108, 1569–1574.
[10] Shimazaki, J., Aiba, M., Goto, E., Kato, N., Shimmura, S. and Tsubota, K. (2002) Transplantation of human limbal epithelium cultivated on amniotic membrane for the treatment of severe ocular surface disorders. Ophthalmology 109, 1285–1290.
[11] Tsai, R.J., Li, L.M. and Chen, J.K. (2000) Reconstruction of damaged corneas by transplantation of autologous limbal epithelial cells. N. Engl. J. Med. 343, 86–93.
[12] Lavker, R.M. and Sun, T.T. (2000) Epidermal stem cells: properties, markers, and location. Proc. Natl. Acad. Sci. USA 97, 13473–13475.
[13] Goodell, M.A., Brose, K., Paradis, G., Conner, A.S. and Mulligan, R.C. (1996) Isolation and functional properties of murine hematopoietic stem cells that are replicating in vivo. J. Exp. Med. 183, 1797–1806.
[14] Goodell, M.A. et al. (1997) Dye efflux studies suggest that hematopoietic stem cells expressing low or undetectable levels of CD34 antigen exist in multiple species. Nat. Med. 3, 1337–1345.
[15] Storms, R.W., Goodell, M.A., Fisher, A., Mulligan, R.C. and Smith, C. (2000) Hoechst dye efflux reveals a novel CD7(+)CD34(−) lymphoid progenitor in human umbilical cord blood. Blood 96, 2125–2133.
[16] Shimano, K. et al. (2003) Hepatic oval cells have the side population phenotype defined by expression of ATP-binding cassette transporter ABCG2/BCRP1. Am. J. Pathol. 163, 3–9.
[17] Jackson, K.A., Mi, T. and Goodell, M.A. (1999) Hematopoietic potential of stem cells isolated from murine skeletal muscle. Proc. Natl. Acad. Sci. USA 96, 14482–14486.
[18] Hulspas, R. and Quesenberry, P.J. (2000) Characterization of neurosphere cell phenotypes by flow cytometry. Cytometry 40, 245–250.
[19] Lechner, A., Leech, C.A., Abraham, E.J., Nolan, A.L. and Habener, J.F. (2002) Nestin-positive progenitor cells derived from adult human pancreatic islets of Langerhans contain side population (SP) cells defined by expression of the ABCG2 (BCRP1) ATP-binding cassette transporter. Biochem. Biophys. Res. Commun. 293, 670–674.
[20] Summer, R., Kotton, D.N., Sun, X., Ma, B., Fitzsimmons, K. and Fine, A. (2003) Side population cells and Bcrp1 expression in lung. Am. J. Physiol. Lung. Cell. Mol. Physiol. 285, L97–L104.
[21] Zhou, S. et al. (2001) The ABC transporter Bcrp1/ABCG2 is expressed in a wide variety of stem cells and is a molecular determinant of the side-population phenotype. Nat. Med. 7, 1028–1034.
[22] Bunting, K.D. (2002) ABC transporters as phenotypic markers and functional regulators of stem cells. Stem Cells 20, 11–20.
[23] Watanabe, K. et al. (2004) Human limbal epithelium contains side population cells expressing the ATP-binding cassette transporter ABCG2. FEBS Lett. 565, 6–10.
[24] Umemoto, T., Yamato, M., Nishida, K., Yang, J., Tano, Y. and Okano, T. (in press). Limbal epithelial side population cells have stem cell-like properties, including quiescent state. Stem Cells.
[25] Budak, M.T., Alpdogan, O.S., Zhou, M., Lavker, R.M., Akinci, M.A. and Wolosin, J.M. (2005) Ocular surface epithelia contain ABCG2-dependent side population cells exhibiting features associated with stem cells. J. Cell. Sci. 118, 1715–1724.
[26] de Paiva, C.S., Chen, Z., Corrales, R.M., Pflugfelder, S.C. and Li, D.Q. (2005) ABCG2 transporter identifies a population of clonogenic human limbal epithelial cells. Stem Cells 23, 63–73.
[27] Pellegrini, G. et al. (2001) p63 Identifies keratinocyte stem cells. Proc. Natl. Acad. Sci. USA 98, 3156–3161.
[28] Mogi, M. et al. (2003) Akt signaling regulates side population cell phenotype via Bcrp1 translocation. J. Biol. Chem. 278, 39068–39075.
[29] Umemoto, T., Yamato, M., Nishida, K., Yang, J., Tano, Y. and Okano, T. (2005) p57(Kip2) is expressed in quiescent mouse bone marrow side population cells. Biochem. Biophys. Res. Commun. 337, 14–21.
[30] Lendahl, U., Zimmerman, L.B. and McKay, R.D. (1990) CNS stem cells express a new class of intermediate filament protein. Cell 60, 585–595.
[31] Seigel, G.M., Sun, W., Salvi, R., Campbell, L.M., Sullivan, S. and Reidy, J.J. (2003) Human corneal stem cells display functional neuronal properties. Mol. Vis. 9, 159–163.
[32] Bhattacharya, S., Jackson, J.D., Das, A.V., Thoreson, W.B., Kuszynski, C., James, J., Joshi, S. and Ahmad, I. (2003) Direct identification and enrichment of retinal stem cells/progenitors by